

**THEORETICAL MODELING OF THE EFFECTS  
OF ROUGHNESS AND GROOVING ON  
THE TRACTION AND FILM HEIGHT  
IN WEB HANDLING SYSTEMS**

**By**

**BENJAMIN ALAN FUNK**

**Bachelor of Science**

**California Institute of Technology**

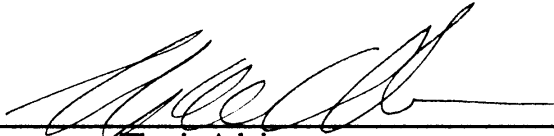
**Pasadena, California**

**1990**

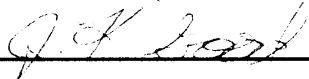
**Submitted to the Faculty of the  
Graduate College of the  
Oklahoma State University  
in partial fulfillment of  
the requirements for  
the Degree of  
MASTER OF SCIENCE  
December, 1993**

THEORETICAL MODELING OF THE EFFECTS  
OF ROUGHNESS AND GROOVING ON  
THE TRACTION AND FILM HEIGHT  
IN WEB HANDLING SYSTEMS

Thesis Approved:



Thesis Adviser



Dean of the Graduate College

## ACKNOWLEDGMENTS

I wish to thank Dr. Frank Chambers for his patience, guidance, and encouragement throughout my graduate studies. Without his help, this research would not have been possible. I also wish to express gratitude to Dr. Peter Moretti and Dr. J. Keith Good for serving on my graduate committee. Their suggestions and support were greatly appreciated. I also wish to express my appreciation to the Web Handling Research Center for its support in my research.

I wish to thank the people at the West Lab for their help during my research there. I would like to especially thank Shermaine King for her friendship and helpful suggestions.

I wish to give my sincere thanks to my parents, Ronald and Marilyn Funk, for their support and direction during my graduate studies. They were always there when I needed help. I would also like to extend my gratitude to my student and other friends here in Stillwater for making my studies here as enjoyable as possible and keeping my life in perspective.

## TABLE OF CONTENTS

Chapter	Page
I. INTRODUCTION . . . . .	1
1.1 Background . . . . .	1
1.2 Review of Foil Bearing Theory for Smooth Roller . . . . .	3
1.2.1 Basic Equations and Assumptions . . . . .	4
1.2.2 Equations for Self-Acting Foil Bearings . . . . .	6
1.2.3 Applications to Web Handling . . . . .	8
1.3 Traction Improvement Mechanisms . . . . .	8
1.3.1 Literature on Roughness and Grooving . . . . .	9
1.4 Possible Sources of Web/Roller Traction . . . . .	11
1.5 Background on Friction . . . . .	11
1.5.1 Factors Affecting Friction . . . . .	12
II. MODELING OF WEB/ROLLER TRACTION . . . . .	15
2.1 Introduction . . . . .	15
2.2 Determination of the Dominant Traction Force . . . . .	15
2.3 Determination of the Mechanism of Reduced Friction (Traction) with Increased Film Height . . . . .	16
2.4 Development of the Traction Model . . . . .	18
2.4.1 Background on Probability . . . . .	18
2.4.2 Application of Probability to the Contact Between Rough Surfaces . . . . .	19
2.4.3 Determination of the Average Traction Force Using Probability . . . . .	21
2.5 Modeling the Various Terms in the Average Traction Force Equation for a Web Handling System . . . . .	21
III. MODELING OF GROOVING EFFECTS ON A WEB/ROLLER SYSTEM . . . . .	25
3.1 Effects of Grooving on a Web/Roller System . . . . .	25
3.2 Basic Grooving Assumptions . . . . .	27
3.3 Development of Grooving Equations . . . . .	28
IV. MODELING FILM HEIGHT OVER A ROUGH ROLLER . . . . .	33
4.1 Discussion of Problem . . . . .	33
4.2 Effects of Roughness on the Film Height . . . . .	34
4.3 Development of an Average Film Height Model . . . . .	36
4.3.1 Assumptions and Basic Equations . . . . .	37
4.3.2 Use of Probability to Determine the Average Height . . . . .	40

V.	FORMULATION OF COMBINED MODELS FOR CALCULATIONS . . . .	42
	5.1 Introduction . . . . .	42
	5.2 First Grooving Approximation-Height Dependent Only . . . . .	43
	5.2.1 Development of Equations . . . . .	43
	5.2.2 Calculations and Results . . . . .	46
	5.3 Second Grooving Approximation-Linear Probability Distribution . . . . .	46
	5.3.1 Development of Equations . . . . .	48
	5.3.2 Calculations and Results . . . . .	52
	5.4 Third Grooving Approximation-Gaussian Probability Distribution . . . . .	52
	5.4.1 Development of Solution for a Generalized Probability Distribution . . . . .	54
	5.4.2 Calculations and Results for the Gaussian Roughness Distribution . . . . .	56
	5.5 Fourth Grooving Approximation-Tension Variation . . . . .	62
	5.5.1 Development of Equations . . . . .	62
	5.5.2 Calculations and Results . . . . .	64
	5.6 Summary . . . . .	66
VI.	CONCLUSIONS . . . . .	68
	6.1 Conclusions . . . . .	68
	6.2 Suggestions for Further Research . . . . .	69
	REFERENCES . . . . .	70
	APPENDIXES . . . . .	72
	APPENDIX A - COMPUTER PROGRAMS . . . . .	73
	APPENDIX B - RAW DATA FROM CALCULATIONS . . . . .	80

## LIST OF FIGURES

Figure	Page
1. Schematic of a Foil Bearing . . . . .	2
2. Various Views of a Foil Bearing Showing the Coordinate System . . . . .	5
3. Flow Regions of a Foil Bearing . . . . .	7
4. Difference Between Real and Apparent Area of Contact . . . . .	13
5. Difference in Pressure in the Air Film for Stationary and Moving Systems . . . . .	17
6. Transverse View of the Constant Gap Regions of a Grooved Roller and an Ungrooved Roller with the Same Film Height . . . . .	26
7. Transverse View of the Constant Gap Regions of a Grooved Roller and an Ungrooved Roller Operating at the Same Conditions . . . . .	29
8. Possible Height Profiles of a Web over a Rough Roller . . . . .	35
9. Transverse View of the Constant Gap Regions of a Smooth Roller and a Rough Roller Operating at the Same Conditions . . . . .	38
10. Transverse View of the Constant Gap Regions of a Web/Roller System Operating at Two Different States . . . . .	44
11. Plot of Groove Fraction versus Velocity Ratio for Various Ratios of Groove Depth to Initial Film Height for the Height Dependent Model . . . . .	47
12. Transverse View of the Constant Gap Regions of a Web/Roller System Operating at Two Different States . . . . .	49
13. Groove Fraction versus Velocity Ratio for Various Ratios of Groove Depth to Initial Film Height for the Linear Probability Distribution . . . . .	53
14. Groove Fraction versus Velocity Ratio for Various Ratios of Groove Depth to Initial Film Height for the Gaussian Probability Distribution . . . . .	57
15. Groove Fraction versus Velocity Ratio for a Groove Depth to Initial Film Height Ratio of 50 for the Three Previous Models . . . . .	58

16. Fractional Change in Groove Fraction from the Height Dependent Model to the Linear Probability Distribution versus Velocity Ratio for Various Ratios of Groove Depth to Initial Film Height . . . . .	60
17. Fractional Change in Groove Fraction from the Height Dependent Model to the Gaussian Probability Distribution versus Velocity Ratio for Various Ratios of Groove Depth to Initial Film Height . . . . .	61
18. Groove Fraction versus Tension Ratio for Various Ratios of Groove Depth to Initial Film Height for the Gaussian Probability Distribution . . . . .	65

## NOMENCLATURE

$a_i$	area of web and roller in contact
$A_{app}$	apparent area of contact between web and roller
$A_{c_{gg}}$	cross-sectional area between a web and a grooved roller above the grooves
$A_{c_{gs}}$	cross-sectional area between a web and a grooved roller above the surface
$A_{cu}$	cross-sectional area between a web and a roller without grooves
$A_{real}$	total real area of contact between web and roller
$b$	one half of the web width
$d$	thickness of web
$f_g$	groove fraction
$\Delta f_g$	change in groove fraction
$f(x)$	distance between the web and roller as a function of the transverse coordinate
$F_f$	friction force per unit area
$F_{ft}$	friction force per unit area causing web/roller traction
$F_n$	normal force between web and roller
$g(k)$	distance between the web and roller as a function of the roller roughness height
$h$	film height
$\Delta h$	change in film height
$h_0$	constant gap film height for smooth roller
$k$	roller roughness height
$L$	length of constant gap region in the direction of web motion
$p$	pressure



$\Delta p$	change in air pressure across the web due to web tension and curvature
$p_a$	ambient air pressure
$p(k)$	probability density function
$p_t$	pressure in air film in constant gap region
$P(k)$	probability distribution function
$r$	radius of curvature of foil
$R$	radius of roller
$s$	coordinate of distance measured along the web in the direction of motion
$T$	tension
$U$	velocity
$w$	width of web/roller cross-section measured across the roller for calculations
$w_g$	total width of grooves in the web/roller cross-section of width $w$
$w_s$	total width of surface in the web/roller cross-section of width $w$
$x$	coordinate of distance measured across the web
$z$	dummy variable used for integration
$\mu$	dynamic viscosity
$\mu_s$	static coefficient of friction
$\theta$	wrap angle

## CHAPTER I

### INTRODUCTION

#### 1.1 Background

Web Handling research has recently become a very important topic for some modern industries. Figure 1 shows a typical web/roller system. With the realization that a thin, lubricating film of air exists between the web and roller, researchers have tried to determine its effects on the web/roller system. Daly (1965) investigated the effects of certain variables on the traction between the web and the roller. He describes a condition which has been observed throughout the paper industry. As the velocity of the web (or roller, if it is the drive roller) increases, more air is entrained into the film between the web and roller. Eventually, enough air builds up to support the web over the roller with no contact between the two surfaces. The end result is that the web and roller lose the traction force which moves them at the same velocity.

Daly found that factors such as tension in the web, speed of the web/roller system, wrap angle, roller diameter, web porosity, and web moisture affect the traction between the web and the roller. His definition of traction was the torque applied by the web on the roller (or vice versa). For all cases, Daly found that increasing the web tension always increased the traction between the web and the roller. Conversely, increasing the speed of the web/roller system always decreased traction due to the increased air film thickness. Roller diameter, however, had a more complex effect on traction. Daly discovered that, for porous webs (webs which air could travel through), the traction would increase as the roller diameter increased. Daly explained this result by stating that the porous webs did not develop a very large air film due to air leaking through the web. As a result, the same force

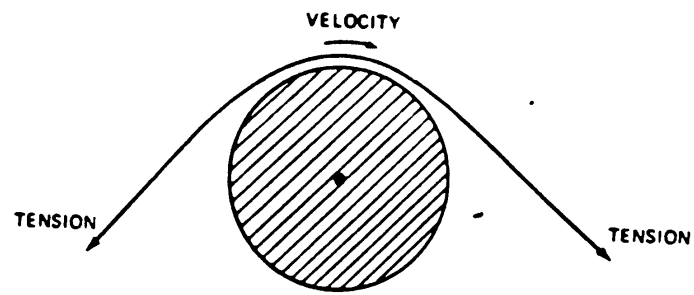


Figure 1. Schematic of a Foil Bearing

(or maybe a larger force due to a larger contact area) between the web and the roller would generate a larger torque due to the increased roller diameter. For nonporous webs, the results were different. The traction decreased as the roller diameter increased. This occurred because larger rollers more easily generate air films, and the extra air could not escape through the nonporous web. Interestingly, Daly found that the traction decreased as porosity increased. Finally, Daly discovered that traction tended to increase as the moisture level increased.

The loss of web/roller traction is a common problem in modern industry due to the very high-speed machinery and can cause many problems. First, maximum efficiency of the machine is not reached since the web may be moving slower than the drive roller. The difference in speeds can also cause damage to the web. The roller roughness asperities still in contact with the web would scrape along the web rather than just pushing into the web surface. Finally, the web could lose lateral traction and drift across the roller. This could impair the operation the machinery (the web enters a certain area incorrectly) or cause the web to drift entirely off the roller.

Knox and Sweeney (1971) were among the first to apply foil bearing theory to the problem of web handling. Previously, the theory had been applied to self-acting foil bearings, in which a thin, flexible medium (the foil) moves over a stationary, rigid surface. Knox and Sweeney extended the analysis to the case where both the foil and the surface were moving at the same velocity. Therefore, a review of foil bearing theory is of interest.

## 1.2 Review of Foil Bearing Theory for Smooth Roller

In a foil bearing, there exists a small, lubricating film between a flexible foil and a more rigid surface. This film is produced by fluid entrainment due to the motion of one or both of the surfaces. The amount of entrained fluid increases as the velocity of the surface(s) in motion increases. This increases the size of the film. The film height is also

dependent on the load forcing the surfaces together. An increase in the load decreases the film height.

### 1.2.1 Basic Equations and Assumptions

The following is taken from the derivation presented more completely in Gross (1980). (Note that R is used to represent roller radius). Barlow (1967a) and Eshel and Elrod (1965), among others, also perform this derivation. Figure 2 shows various views of the foil bearing.

Gross presents the Reynolds equation for a foil bearing with his choices of variables as follows.

$$\frac{\partial}{\partial x} \left( h^3 p \frac{\partial p}{\partial x} \right) + \frac{\partial}{\partial s} \left( h^3 p \frac{\partial p}{\partial s} \right) = 6\mu U \frac{\partial(ph)}{\partial s} + 12\mu \frac{\partial(ph)}{\partial t} \quad (1-1)$$

For an infinitely wide, perfectly flexible foil with an incompressible lubricant and time-steady characteristics, the derivatives with respect to x and t are zero, and the pressure derivative with respect to s is much smaller than the pressure itself.

If the film height h is small compared to the radius of the roller, the radius of the roller can be used to approximate the radius of curvature of the foil. The following equilibrium equation for a foil bearing is derived by Barlow (1967a).

$$\frac{Et^3}{12(1-\nu^2)} \nabla^2 \nabla^2 h + \frac{Et(h-h_0)}{R^2} = p - p_0 - \frac{T}{R} \left( 1 - R \frac{\partial^2 h}{\partial s^2} \right) \quad (1-2)$$

For the perfectly flexible foil, the bending term can be neglected (left hand side of the equation). Combining the two simplified equations yields:

$$\frac{\partial}{\partial s} \left( h^3 \frac{\partial^3 h}{\partial s^3} \right) = \frac{-6\mu U}{T} \frac{\partial h}{\partial s} \quad (1-3)$$

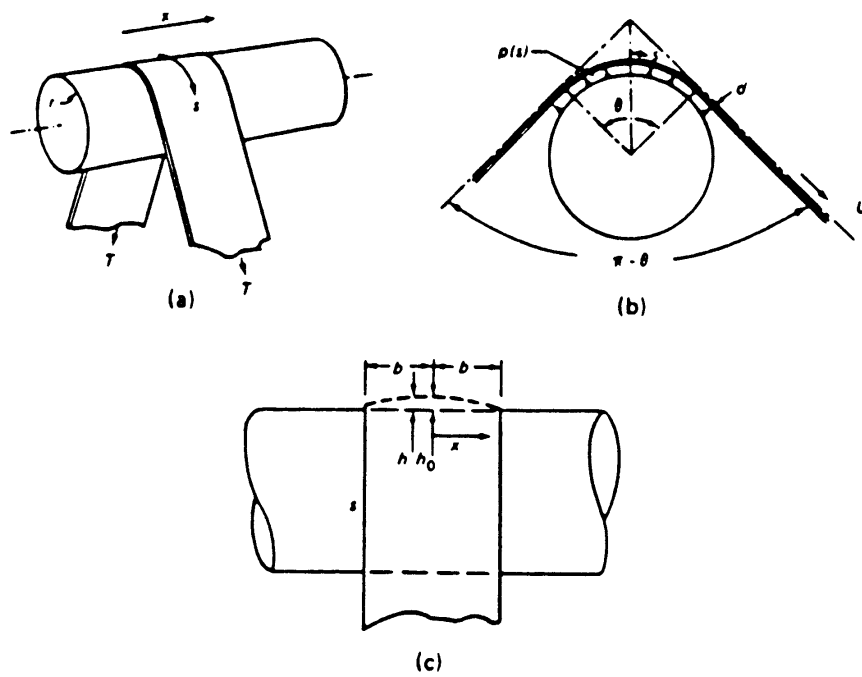


Figure 2. Various Views of a Foil Bearing Showing the Coordinate System (Gross, 1980)

This is the foil bearing equation. Gross develops dimensionless variables for the equation and uses them to make the equation nondimensional. He then integrates the equation once and performs a simple linearization to obtain a solution. The solution predicts three regions for the foil bearing with different equations operating in each. Figure 3 shows a diagram of these regions.

The first region in the figure is the entrance region. In this region, the pressure in the air film increases with the decreasing gap height. From the solution, the decrease in gap occurs smoothly and is exponential in form. The second region is the constant gap region. In this region, the air film height and the pressure are constant. Thus, there are no pressure gradients or effects of pressure gradients on the fluid flows in the constant gap region. As a result, the flow in the bearing is solely a Couette flow, and information can therefore only be transmitted in the direction of relative surface motion. Thus, conditions at the entrance always determine downstream behavior. The final region is the exit region. In this region, the gap decreases to some minimum height and then starts to increase. This behavior is sinusoidal in nature. These regions exist for all foil bearings.

### 1.2.2 Equations for Self-Acting Foil Bearings

The infinitely wide, perfectly flexible, self-acting foil bearing has been of particular interest. For this case, the foil is moving at some velocity,  $U$ , while the surface is kept stationary. Investigations have been made by Baumeister (1963), Eshel and Elrod (1965), and Barlow (1967b). Ma (1965) and Licht (1968) have conducted experimental analyses of self-acting foil bearings. Of primary concern has been the film height of the bearing in the constant gap region, although Barlow was also interested in the minimum gap between the web and the roller. Further, Eshel and Elrod produced a numerical solution for the entrance and exit regions. Gross investigated the assumptions made in the derivation to determine the ranges of the various parameters for which the assumptions would hold. For self-acting foil bearings, the air film height is given by the following equation:

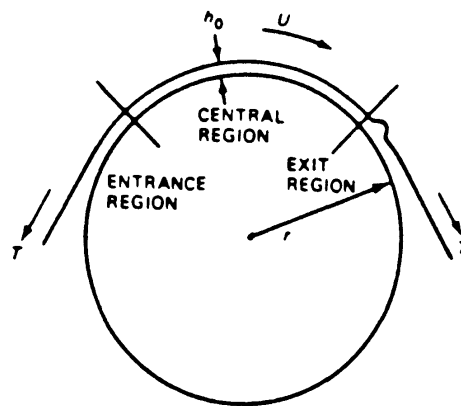


Figure 3. Flow Regions of a Foil Bearing (Gross, 1980)



$$\frac{h_0}{R} = K \left( \frac{6\mu U}{T} \right)^{\frac{2}{3}} \quad (1-4)$$

The generally accepted value for the constant, K, is 0.643, although other possible values have been presented (cf. Baumeister (1963)).

### 1.2.3 Applications to Web Handling

Knox and Sweeney (1971) proposed a change to Equation (1-4) that would allow its application to web handling research. Their studies involved a flexible web (foil) moving over a rotating roller (surface) such that both were moving at the same velocity. They contended that, for a system in which both the foil and the surface were in motion, the proper form for equation (1-4) would be:

$$\frac{h_0}{R} = 0.643 \left( \frac{12\mu U}{T} \right)^{\frac{2}{3}} \quad (1-5)$$

This has been expanded into the more general form used in this thesis:

$$\frac{h_0}{R} = 0.643 \left[ \frac{6\mu(U_{web} + U_{roller})}{T} \right]^{\frac{2}{3}} \quad (1-6)$$

## 1.3 Traction Improvement Mechanisms

There are currently two prevalent methods used to increase web/roller traction to acceptable levels. The first involves increasing the surface rms roughness of the roller. Contact between roughness asperities appears to be a major factor in web/roller traction. An increase in roughness rms will increase the number of roller asperities that penetrate the air film, thus improving traction. However, caution must be exercised. If the roughness

asperities are too large, they might damage the web even without slip between the two surfaces. This will occur as the web, assumed perfectly flexible, deforms around the peaks due to the tension in the web. So it is not always desirable to increase traction in this manner.

The second prevalent method of increasing web/roller traction is to groove the roller surface. These grooves help to transport the air entrained by the web and the roller. As a result, they may lower the film height over the ungrooved portion of the roller. Since the web is closer to the roller in these sections, there will be increased asperity contact which will result in more traction. However, the grooves must be designed so that the increase in traction is greater than the loss in traction due to the grooved section being farther from the web. Also, care must be taken to choose a groove pattern which will not "wrinkle" or damage the web.

With no analytical way of solving these problems, the industries have used empirical methods. This usually involves trial and error. As a case of deficient traction arises, a roller is either roughened or grooved in a certain manner. Then, it is mounted to the machine and tested to see if it corrects the problem. If it works, it must then be determined if the new configuration causes unacceptable damage to the web or other problems to the system. If the problem still exists or the roller is otherwise unacceptable, a new grooved or roughened roller must be prepared. This continues until all conditions have been satisfied.

### 1.3.1 Literature on Roughness and Grooving

The effect of roughness and grooving on the fluid film in bearings has been a major topic of study, especially with respect to the load carrying capacity of the bearing. Patir and Cheng (1978,1979) used an average Reynolds equation to model the flow past rough surfaces. They use pressure and shear flow factors to account for the changes in the flow due to the presence of roughness. White (1980,1983), Christensen and Tondor (1971),

and Tondor (1980,1984,1985a, 1985b) have also investigated this area. Chengwei and Linqing (1989) use the model from Patir and Cheng but modify the combined roughness distribution of the surfaces with a contact factor. Chang and Webster (1991) use elastohydrodynamic analysis to model the roughness effects. Elrod (1973) studied the effects of grooves on the lubrication of bearings. The studies, however, have mainly been concerned with bearings in which there is flow past the roughness. This is not true in the constant gap region for web handling, where there is no pressure gradient or relative velocity between the web and the roller. Also, web handling research is primarily concerned with the traction between the web and the roller rather than the load bearing capacity. So, while these analyses are not directly applicable to web handling traction problems, they are of interest.

There is some disagreement as to the effects of roughness on the load carrying capacity of bearings. The theory of Christensen and Tondor (1971) predicts a decrease in load carrying capacity with an increase in surface roughness. Conversely, White (1980,1983) developed a model which predicts an increase in load carrying capacity with an increase in roughness. White contends that the closure assumption used by Christensen and Tondor breaks down at large bearing numbers. The bearing number depends on the ratio of the dynamic viscosity times the relative velocity of the bearing surfaces in the direction of motion and the length scale in the direction of motion to the ambient air pressure times the constant gap film height squared. It is difficult to determine the applicability of these models to a web handling system with no relative motion between the surfaces (a bearing number of zero), but both point to strong roughness effects on bearings with very thin, compressible lubricants.

However, roughness magnitude is not the only roughness characteristic which affects pressure or shear flow past a roughened surface. The orientation of the surface roughness with respect to the main flow can also have an effect. Patir and Cheng (1978,1979), among others, state that if the roughness is mainly oriented parallel to the

primary flow, the shear or pressure flow is enhanced by the roughness. The roughness directs the fluid in the direction of the primary flow and restricts any side flow. However, if the roughness orientation is transverse to the primary flow or isotropic, it will restrict the pressure or shear flow. In this case, the roughness blocks fluid from traveling in the direction of the primary flow and creates more side flow. Thus, the roughness orientation also affects the flow past roughened surfaces.

#### 1.4 Possible Sources of Web/Roller Traction

The most obvious contribution to web/roller traction comes from the contact friction between the two surfaces. This is caused by the roughness asperities from the web and the roller piercing the air film to make contact with each other. The tension in the web provides a normal force (or load) between the surfaces which would cause friction. In fact, if both the web and the roller were stationary, the friction force would be easily computable. However, as the web and roller start to move, the friction contribution becomes more difficult to quantify.

A second contribution could come from a viscous shear stress in the air film itself. If there were a velocity gradient in the entrained air between the web and the roller, it would cause a shear stress acting on the two surfaces. This shear stress only exists if the two surfaces are moving at different velocities and acts to keep the two surfaces moving at the same velocity.

Also, in light of some experience in the lab, certain other factors, especially static electricity, should not be ruled out as a contribution to traction. It has been observed that a large amount of static electricity can cause a considerable adhesion force between two surfaces. Another possible factor is that impurities can build up between the web and the roller, either brought in by the entrained air or worn off of the roller or the web. These impurities could alter the friction force between the two surfaces, acting similar to a second lubricating film. Either of these could have an effect on the traction in a web/roller system.

## 1.5 Background on Friction

Bhushan, Sharma, and Bradshaw (1984a,1984b) made an extensive study of the friction in magnetic tapes. Since magnetic tapes moving over stationary heads resemble self-acting foil bearings, this study was of interest. Although the results are not perfectly applicable to the web handling traction problem, many of the factors which can affect friction between flexible and rigid surfaces are discussed. These provide insight for determining the friction force between the web and the roller when both are in motion.

### 1.5.1 Factors Affecting Friction

From a review of literature on friction, it is found that friction occurs between two surfaces when there is a force (load) pressing the two surfaces together. The common theme among the references (Rabinowicz (1965), Sarkar (1980), Kragelskii (1965), Bhushan (1984)) is that the amount of friction between two surfaces is dependent on the real area of contact between the two surfaces. The real area of contact is defined as the area of the two roughened surfaces that is in actual contact. Figure 4 illustrates the difference between the real area of contact and the apparent area of contact of two surfaces. The real area of contact depends on certain factors. It depends on the physical properties of the two substances involved (malleability, roughness characteristics, etc.). It also depends on the normal force or load pushing the surfaces together.

From the literature, it is found that the real area of contact between two surfaces is directly proportional to the normal force between the surfaces. It is not related to the apparent area of contact between the surfaces. Therefore, a reduction in normal force causes a reduction in friction even if the apparent area of contact remains the same. The effect of the properties of the two substances is more difficult to ascertain. A more malleable substance could deform around the other surface at points of contact, generating a larger real area of contact. Roughness asperities could interlock, making it more difficult to cause relative motion between the surfaces. These effects are usually combined into an

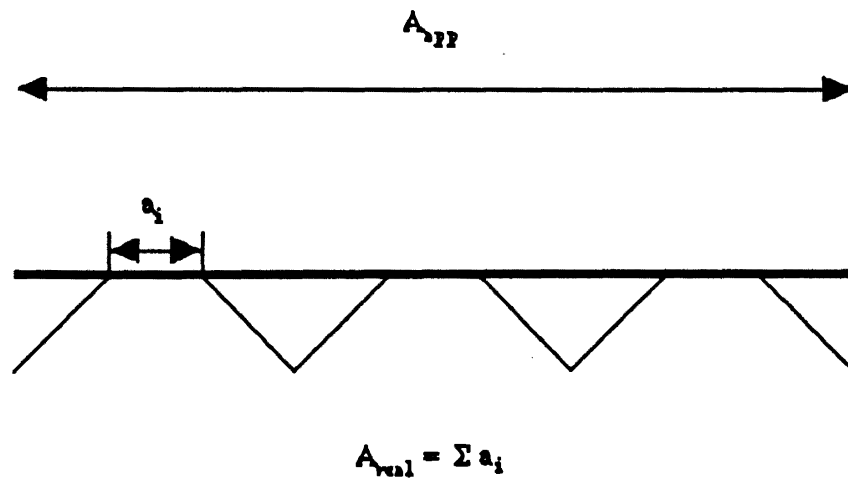


Figure 4. Difference Between Real and Apparent Area of Contact

empirically determined friction coefficient. There are two friction coefficients. The static coefficient of friction represents these effects when the two surfaces are at rest with respect to each other, and the dynamic coefficient of friction represents these effects when there is relative motion between the two surfaces. In this thesis, it is assumed that there is always perfect traction and no relative motion between the web and the roller. Thus, the static coefficient of friction will be used for the models.

## CHAPTER II

### MODELING OF WEB/ROLLER TRACTION

#### 2.1 Introduction

Before predictions about the effects of roughness and grooving on traction can be made, a model of web/roller traction for rough rollers must be developed. To make such a model, one must first discover what is producing the traction force. From this, the factors which affect the traction force and, thus, the mechanism for the reduction of traction with increased film height can be determined. One can then determine and model the effects of the roller roughness on web/roller traction.

#### 2.2 Determination of the Dominant Traction Force

For the following model, it will be assumed that the web and roller are operating under conditions of perfect traction. Perfect traction occurs when there is no slip between the web and the roller (i.e., the web and the roller are moving at the same velocity). As a result, there is no velocity gradient in the constant gap region of the air film (where there is no pressure gradient). Also, it will be assumed that, even in regions where there is a pressure gradient, the resulting viscous shear stress is small enough that it is negligible compared to the contact friction. Finally, the contribution to traction from other factors, such as static electricity, will be ignored. While static electricity can be a primary contributor to traction, its effects are difficult to quantify. Thus, the effects of static electricity will be ignored to simplify the development of this model. This leaves contact friction as the dominant force affecting web/roller traction.



### 2.3 Determination of the Mechanism of Reduced Friction (Traction) with Increased Film Height

How the surfaces bend and react to one another can greatly affect the friction force created between them in a web/roller system. Also, when the two surfaces are stationary with respect to one another, the asperities of the two surfaces can interlock, increasing the amount of force necessary to cause relative motion between the surfaces. However, if the same two substances are used at every velocity, the traction still decreases. This means that the actual surface properties are not causing the reduction in traction. Moreover, the web asperities are, in general, much smaller than the roller asperities. This, combined with the assumption that the web is perfectly flexible, should reduce the effects of interlocking asperities on traction in the case of the web/roller system. This leaves a change in effective load between the two surfaces as the only cause for a loss of traction.

If the web/roller system is examined, it is found that at zero velocity for the web and roller, there is no entrained air between the two surfaces. Any air between the two surfaces is at atmospheric pressure, and, thus, all of the load from the tension in the web is supported by the roller as illustrated in Figure 5a. However, as the web and roller start moving, a pressurized air film develops between the two. This air film lifts the web off the roller, so it must be supporting some of the load from the tension in the web as shown in Figure 5b. The effect of this is to reduce the load created by the contact between the web and roller. From the references (Rabinowicz (1965), Sarkar (1980), and Kragelskii (1965)) on friction, the reduced load between the web and the roller decreases the friction force between the web and the roller. And, since the friction between the web and the roller is the main source of traction between the two, the traction is also reduced. This analysis is also forwarded by Jones (1992).



(a) web and roller stationary



(b) web and roller in motion ( $p > p_a$ )

Figure 5. Difference in Pressure in the Air film for Stationary and Moving Systems

## 2.4 Development of the Traction Model

The mechanism for the reduction of traction in the web/roller system due to increased air film thickness has been determined, but it is still necessary to construct a model that uses this information to predict the amount of traction at a given film height. From the investigation, it is known that the only contributions to traction come from points at which the web and roller are in contact. At all other points, the web is supported by the air film. However, it is extremely difficult to determine exactly the amount of contact between the web and roller. This would require knowledge of the film and roughness heights everywhere over the web and the roller. Also, the film height and roughness characteristics change as the web and roller move. The resulting calculations would be extremely complex. However, the paper by Patir and Cheng (1978) suggests a possible approach when it uses an average flow model to account for the roughness in the system. This allows results to be found in general for the entire system without specific information or time dependence.

### 2.4.1 Background on Probability

In mathematics and physics, probability is often used as a way of determining the average result of certain problems. It is also used in turbulence calculations to give an average value for a system which is continuously fluctuating. In a similar manner, probability density and probability distribution functions can be applied to the roller roughness. Both Tondor (1980) and Chengwei (1989) have used probability to model the roughness for their calculations. While this does not reveal if the roughness at a certain point on the roller's surface pierces the air film to make contact with the web, it indicates the chance that such contact would occur. For example, assume that a certain roller has a probability density function  $p(k)$  and an associated probability distribution function  $P(k)$ , where  $k$  is the height of the roughness on the roller surface.  $P(k)$  is defined as follows:

$$P(k) = \int_{-\infty}^k p(z) dz \quad (2-1)$$

By definition,  $p(k)$  is the probability that the roller roughness will be equal to height  $k$  and  $P(k)$  is the probability that the roller roughness will be less than or equal to height  $k$ . By definition,  $P(k)$  has the property:

$$P(\infty) = \int_{-\infty}^{+\infty} p(z) dz = 1 \quad (2-2)$$

In words, this means that if all the probabilities are summed over the entire range of  $k$ , the result is one. From this line of reasoning, it is known that the sum of the probability of the roughness height being less than or equal to  $k$  and the probability of the roughness height being greater than or equal to  $k$  is one since the entire domain of roughness heights is covered (the height must be less than, equal to, or greater than  $k$ ). So,

$$P(k) + P^*(k) = 1 \quad (2-3)$$

where  $P^*(k)$  is the probability that the roughness height is greater than or equal to  $k$ . Or, in another form:

$$P^*(k) = 1 - P(k) \quad (2-4)$$

#### 2.4.2 Application of Probability to the Contact Between Rough Surfaces

Equation (2-4) is very useful. For example, it is known that the air film thickness at certain point in the web/roller system is  $h$  (measured from the same point of reference as

the roughness distribution). For traction purposes, it is desirable to know if the web and roller are in contact at this point. For the web and roller to be in contact, the roughness must pierce the air film. This would occur only if the roughness height at that point is greater than or equal to  $h$ . The probability of this occurring is  $P^*(h)$  (or  $1-P(h)$ ). It is from this relationship that the traction model will be derived.

It should be noted that this relationship is only true if the chance of contact between the web and the roller at a point is dependent only on the roughness at that point. This is not always the case. It has been observed that two rollers with the same roughness distribution can have different traction characteristics. This is because the contact between the web and the roller depends on the roughness magnitude and the roughness wavelength (how quickly the roughness changes). This is more fully discussed in the section on developing the height model. For now, it will be assumed that the roughness distribution has characteristics which cause the probability of contact at a point to be independent of the roughness of the surrounding points.

#### 2.4.3 Determination of the Average Traction Force Using Probability

For a given web/roller system with a rough roller, the height of the web above the roller at a point  $(x,s)$  is given by  $h(x,s)$  where  $s$  is the direction along the roller and  $x$  is the direction across the roller. Once again,  $1-P(h)$  is the probability that the roughness touches the web at that point.  $F_n(x,s)$  is the normal force per unit area which would be exerted between the two surfaces if they were in contact at the point. Thus, the average normal force per unit area exerted between the web and the roller at this point is:

$$\overline{F}_n(x,s) = \{1 - P[h(x,s)]\}F_n(x,s) \quad (2-5)$$

The bar over the  $F$  on the left hand side of the equation denotes the time averaged force.

Further, if the static coefficient of friction between the two surfaces is  $\mu_s$ , then the average friction force per unit area (the contributor to traction between the surfaces) is:

$$\overline{F}_f(x,s) = \mu_s \{1 - P[h(x,s)]\} F_n(x,s) \quad (2-6)$$

To determine the total average friction force for the system, Equation (2-6) must be integrated over the entire domains of  $x$  and  $s$ . This yields:

$$\overline{F}_{f_t} = \int \int \mu_s \{1 - P[h(x,s)]\} F_n(x,s) ds dx \quad (2-7)$$

## 2.5 Modeling the Various Terms in the Average Traction

### Force Equation for a Web Handling System

Equation (2-7) can be used to model the average friction force (i.e., traction) generated by the web/roller system if the coefficient of friction, the air film height, the normal force per unit area, and the roller roughness height probability distribution are known. The difficulty now lies in determining the appropriate values for these variables.

The coefficient of friction between the surfaces is the easiest to model. There are two possible options for the web/roller system. The first possibility is that there is no relative motion between the web and the roller. The friction force would then be computed as if the two were stationary with respect to one another. The proper term would thus be the static coefficient of friction. Conversely, if there were relative motion between the surfaces, the dynamic coefficient of friction would be used. For the calculations made here, it is assumed that perfect traction exists and there is no relative motion between the web and the roller. So, the static coefficient of friction will be used.

Next, the normal force per unit area must be determined. From Gross' (1980) derivation, it is known that the change in pressure across the web is related to the tension in the web and the radius of curvature of the web. The equation is:

$$\Delta p = \frac{T}{r} \quad (2-8)$$

This is the amount of air pressure needed to support the tension in the web at a point. The total pressure under the web would then be:

$$p_t = p_a + \Delta p = p_a + \frac{T}{r} \quad (2-9)$$

where  $p_a$  is the ambient pressure of the air. This total pressure is the force per unit area required to hold the web above the roller. Thus, this would be the force per unit area pushing the web onto the roller if the two were in contact (the force the roller would have to support if the two were in contact). So, for a system running under the assumptions that Gross uses in his derivation (web is infinitely wide and perfectly flexible), the normal force per unit area would be:

$$F_n(x,s) = p_a + \frac{T}{r} \quad (2-10a)$$

(Note:  $r$  is a function of  $x$  and  $s$ .) The pressure term is usually small compared to the tension term, so it will be neglected. This leaves:

$$F_n(x,s) = \frac{T}{r} \quad (2-10b)$$

To do the following calculations, it will be assumed that the traction for the web/roller system comes primarily from the constant gap region. The contributions from the other regions will be ignored. Further, in this region, it will be assumed that the height of the web over the reference point where the web roller roughness has zero mean is equal to the air film height for the constant gap region computed by the foil bearing equation. The reason for this is that, at the heights at which traction could be lost, only the

largest roughness asperities pierce the air film to make contact with the web. So, if the roughened roller transports the same amount of air as the smooth roller, the extra air transported by the roughness valleys should almost equal that blocked by the roughness peaks, and the film height would then be approximately that computed by the foil bearing equation.

These assumptions simplify the general equation greatly. With them, the general term  $h(x,s)$  can be replaced by the constant film height computed by the foil bearing equation. Also, the radius of curvature from the normal force equation is also a constant. A further, very good assumption that the film height is much smaller than the roller radius (as in Gross' derivation) simplifies the normal force equation even further. In this case, the film height can be neglected and the radius of curvature is just the radius of the roller. Substituting into the traction force equation yields:

$$\overline{F}_{t_t} = \int \int \mu_s \{1 - P(h_0)\} \frac{T}{R} ds dx \quad (2-11)$$

Since none of the terms in this equation depend on  $x$  or  $s$ , they can be moved outside the integral. This results in the equation:

$$\overline{F}_{t_t} = \mu_s \{1 - P(h_0)\} \frac{T}{R} \int \int ds dx \quad (2-12)$$

The extent of the constant gap region in the  $s$  direction will be assumed to be  $L$ . Thus,

$$\overline{F}_{t_t} = \mu_s L \{1 - P(h_0)\} \frac{T}{R} \int dx \quad (2-13)$$

Equation (2-13) models the average traction force of a web/roller system operating under the current assumptions. Calculations of the average traction force can be made



without detailed knowledge of the roller roughness if the static coefficient of friction, length of constant gap region, roller roughness probability distribution, air film height, web line tension, roller radius, and web width are known. Furthermore, comparisons of the traction force of a web/roller system operating at two different states can be made.

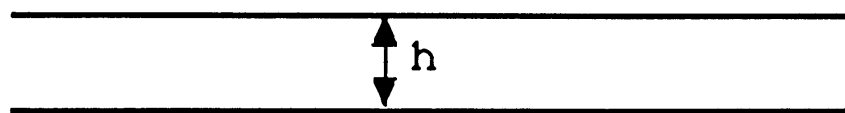
## CHAPTER III

### MODELING OF GROOVING EFFECTS ON A WEB/ROLLER SYSTEM

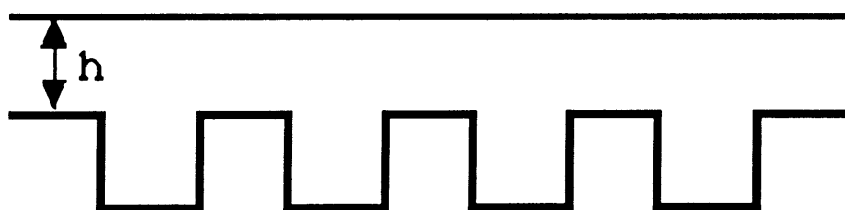
#### 3.1 Effects of Grooving on a Web/Roller System

Grooving rollers is a prevalent method of increasing web/roller traction. However, the manner in which the grooves increase traction must be determined before a model can be developed. To discover this, one must examine the web/roller system with and without grooves and observe the effects of the grooves on the system.

An important characteristic of the web/roller system that affects traction is the height of the entrained air film between the web and the roller. The web and the roller transport air between them as shown in Figure 6a. The amount of air transported is related to the cross-sectional area between the web and roller. An increase in web/roller velocity increases the amount of entrained air. The increase in entrained air increases the film height (and thus the cross-sectional area) between the web and the roller. Now, add circumferential grooves to the roller and run the system with the same conditions as before without grooves. If the film height above the surface is assumed to be the same as for the roller without grooves, the system would look like Figure 6b. This system has more cross-sectional area between the web and the roller and, thus, transports more air than the system without grooves. However, since both systems run at the same conditions, a plausible first approximation might be that they transport the same amount of air. For this to be true, the film height over the surface of the grooved roller would have to be smaller than for the ungrooved roller. Empirically, it is known that traction increases as the



(a) roller without grooves



(b) roller with grooves

**Figure 6. Transverse View of the Constant Gap Regions of a Grooved and an Ungrooved Roller with the Same Film Height**

film height decreases. Thus, the cause for the increased traction for the grooved rollers may be that the film height over the surface of the roller is less than that for the ungrooved roller. This increase overcomes the decrease of traction over the grooves due to the increased film height there.

### 3.2 Basic Grooving Assumptions

The central assumption made in modeling the effects of grooving on the web/roller system is that the grooved and ungrooved rollers transport the same amount of air. Or, more accurately, that the grooved roller transports the same amount of air as an ungrooved roller at that same set of conditions if the ungrooved roller had perfect traction. Also, it is assumed that cross-sectional area can always be used as the measure of this air transport. This is not necessarily true, especially at low velocities and film heights. A real web cannot follow the surface of the roller perfectly. There will be a gaps in certain areas in the grooves where the web cannot touch, even with no entrained air. Until these gaps are filled, the web will not rise out of the groove. Thus, the cross-sectional area of grooved roller under such conditions would be larger than for an ungrooved roller, even if the amount of air entrained by the two were the same. However, for purposes of the calculations presented here, it will be assumed that conditions are such that both the grooved and ungrooved rollers transport the same amount of air.

Another major assumption made for these calculations is that the web lies flat above the grooved roller. This is not necessarily valid. At low film heights, the perfectly flexible web will tend to follow the surface of the roller and dip into the grooves. For the web to remain flat above the entire roller, the entrained air would have to distribute itself into the grooves in some manner. Even then, at low velocities, the amount of entrained air could still be less than the amount the grooves can transport, and the web would still dip into the grooves on the roller. However, to simplify the following calculations, it is assumed that the web lies flat above the grooved roller.

The final assumption made is that the roller surface roughness has no effect on the air film height above the surface of the roller. For small air film heights, this is not the case. Whether the web follows the roller roughness or only makes contact with the roller roughness asperities, the roughness has a definite effect on the air film height. As a first approximation, however, the effect of roller roughness on the web air film height will be neglected.

### 3.3 Development of Grooving Equations

Assume that a web/roller system is operating at a certain set of conditions (velocity, tension, etc.). If perfect traction exists, the film height in the constant gap region for a smooth roller can be determined from Equation 1-5.

$$\frac{h_0}{R} = 0.643 \left( \frac{12\mu U}{T} \right)^{\frac{2}{3}} \quad (3-1)$$

A sketch of this system appears in Figure 7a. Grooves are then added to the roller, and the system is run at the same conditions. The system now looks like that illustrated in Figure 7b.

One nondimensionalized variable is introduced to simplify matters before the calculations are made. This is the groove fraction ( $f_g$ ), which is the fraction of the roller surface that is taken up by the grooves. Combined with the groove depth, it determines the amount of air transported by the grooves. This value has an upper limit of 0.5 for logical reasons. At that point and beyond, there is a question of whether the top or the bottom of the grooves is the "real" surface of the roller. The roller may be perceived as either a roller with a large amount of grooving or a roller with certain areas raised above the rest of the surface. The calculations would, therefore, cease to have meaning for groove fractions greater than 0.5. For the section of width  $w$ , the groove fraction is assumed to be the same as for the entire roller. This groove fraction can be expressed as:

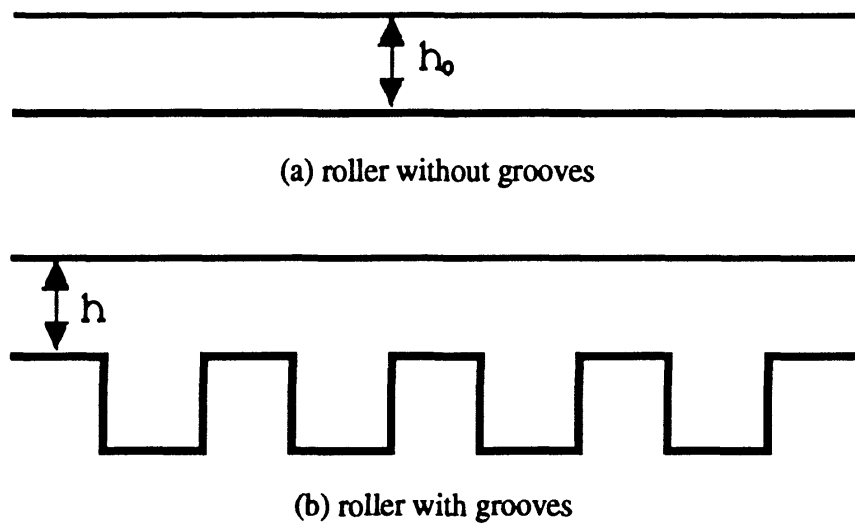


**Figure 7. Transverse View of the Constant Gap Regions of a Grooved Roller and an Ungrooved Roller Operating at the same Conditions**

$$f_g = \frac{w_g}{w_g + w_s} \quad (3-2)$$

$w_g$  =total width of grooves in section

$w_s$  =total width of surface in section

Since there is no other part in the section that is not groove or surface, the sum of width of the grooves and surface must be the total width of the section,  $w$ . Thus:

$$f_g = \frac{w_g}{w} \quad (3-3)$$

From the assumptions, both the grooved and ungrooved rollers at the same condition transport the same amount of air (the amount of air transported by a smooth roller at the state with perfect traction). This amount of air transported is proportional to the cross-sectional area between the web and the roller. For the case of the ungrooved roller, this is easily computed for a section of width  $w$  as:

$$A_{c_u} = h_0 w \quad (3-4)$$

For the grooved roller, it is a little different. The calculation is split into two parts for the area above the surface and the area above the grooves. The height above the surface for the grooved roller is  $h$ , so the total cross-sectional area between the web and the surface is:

$$A_{c_g_s} = w_s h \quad (3-5)$$

Similarly, the film height over the grooved part of the roller is  $h+d_g$ , so the total cross-sectional area between web and grooves is:

$$A_{c_{g_g}} = w_g(h + d_g) \quad (3-6)$$

The total cross-sectional area for the grooved roller is the sum of these two parts. For the cross-sectional area of the grooved and ungrooved rollers to be the same:

$$A_{c_{g_u}} + A_{c_{g_g}} = A_{c_u} \quad (3-7a)$$

Or,

$$w_u h + w_g(h + d_g) = wh_0 \quad (3-7b)$$

This equation has three variables ( $w_u$ ,  $w_g$ , and  $d_g$ ). It would be convenient if this could be reduced to two variables. This is relatively simple since it is known that:

$$w_u + w_g = w \quad (3-8a)$$

Or,

$$w_u = w - w_g \quad (3-8b)$$

Substituting this into the equation yields:

$$(w - w_g)h + w_g(h + d_g) = wh_0 \quad (3-9)$$

Expanding all terms:

$$wh - w_g h + w_g h + w_g d_g = wh_0 \quad (3-10)$$



Simplifying:

$$wh + w_g d_g = wh_0 \quad (3-11)$$

Dividing through by w:

$$h + \frac{w_g}{w} d_g = h_0 \quad (3-12)$$

One term in the equation can be recognized from Equation (3-3) as the groove fraction.

Substituting yields:

$$\begin{aligned} h + f_g d_g &= h_0 \\ h &= h_0 - f_g d_g \end{aligned} \quad (3-13)$$

Equation (3-13) expresses the air film height of the constant gap region over the surface of the grooved roller in terms of the air film height in the constant gap region of an ungrooved roller operating at the same conditions, the groove fraction, and the groove depth. It is important to remember that this equation only holds if the roller is smooth or if the roller roughness is assumed to have no effect on the air film height. However, this model will be used as a first approximation of the effects of grooving on the air film height of a web/roller system.

## CHAPTER IV

### MODELING FILM HEIGHT OVER A ROUGH ROLLER

#### 4.1 Discussion of Problem

All traction calculations presented so far have been made assuming that the film height measured from the point at which the roughness distribution has zero mean for the roughened roller could be computed using the foil bearing equation developed for a smooth roller. As has been stated previously, this assumption is not necessarily valid, especially for small film heights where there is significant contact between the web and the roller. If the smooth and rough rollers are assumed to transport the same amount of air, the roughness valleys would act like very small grooves on the roller's surface. These valleys would transport more air and thus lower the film height over the roller. Conversely, the roughness peaks will more often be in contact with the web and would transport less air. At large film heights, these effects almost balance out, but this is not true at small film heights. So, to determine a more accurate film height for a roughened roller, a height model should account for these effects.

Once again, as for the traction force, it is difficult to determine the height of the web over the roller at a specific point. Because the roughness changes as the roller rotates, the web height over the roller varies with time as well as position. Very detailed knowledge of the roughness would be necessary to find the exact film height everywhere as a function of time and position, and the solution would be very complex. However, determining a time-averaged film height at a certain point would eliminate one of the variables. There is a loss of accuracy since, similar to the average traction force, the actual film height at a given

time fluctuates about the average height, but this will be sacrificed for simplicity in computation.

#### 4.2 Effects of Roughness on the Film Height

A major problem in creating a film height model is determining the effects of the roughness on the air film. For the traction model, it was a matter of examining the forces between the web and the roller and finding the mechanism which reduced traction as the film height increased. For the height model, it is not that simple. Smooth and roughened rollers might not transport the same amount of air. Further, the web might not be able to follow the surface of the roller closely due to the roller roughness, web flexibility, or web thickness. These factors must be examined before a model can be made.

First, for large film heights, there is not much difference between smooth and rough rollers. If the film height is much larger than the surface roughness rms, the effects of the roughness on the developed air film are negligible since the amount of air transported near the surface of the roller is very small compared to the total air transported. Thus, for these conditions, the amount of air transported and the film height for the rough roller can be assumed to be approximately the same as those for a smooth roller. So, as the film height increases, the film height for the roughened roller must start to approach that for the smooth case at a certain point. The problem now is to determine the film height for the rough roller for those cases where the roughness does affect the air transport.

The next problem is determining whether or not the smooth and rough rollers transport the same amount of air in regions where the roughness is not much smaller than the film height. This is affected by the facility with which the web should be able to follow the surface of the roller. If the roller roughness has a relatively large wavelength with respect to the thickness and flexibility of the web and the rms of the surface roughness, then the web can follow the surface of the roller fairly closely as illustrated in Figure 8a. For this case, the smooth and rough roller may transport the same cross-sectional area of



(a) web follows roller roughness



(b) web and roller only in contact at asperities

**Figure 8. Possible Height Profiles of a Web over a Rough Roller**

air. However, if the roller roughness wavelength is small enough, the web will tend to touch the roller only at the roughness peaks and will not dip into the valleys as shown in Figure 8b. The rough roller will not transport the same cross-sectional area of air as the smooth roller for this case. The two cases will be examined separately.

For the first case, the web and roller are in contact everywhere at zero velocity. As the web/roller system starts to move, an air film develops between the web and the roller. This air film lifts the web off portions of the roller, leaving other areas still in contact. The cross-sectional area of the transported air could therefore be equal to that for the smooth roller operating at the same conditions. As the velocity increases, the amount of contact between the web and roller decreases until only the largest roughness asperities are in contact with the web. When the velocity increases even further, the web and the roller are no longer in contact.

The second case is slightly different. For this case there is area between the web and the roller even at zero web/roller velocity. As the pressurized air film develops, it will partially distribute itself into the gaps already present between the web and the roller. So, until enough air is entrained, the web will not change greatly from its initial position above the roller. Thus, at the lower web/roller velocities, there will be a larger cross-sectional area between the web and the rough roller than for the smooth roller operating at the same conditions. As the amount of entrained air increases, the cross-sectional area for the rough roller will approach that of the smooth roller and that of the first case.

#### 4.3 Development of an Average Film Height Model

For real systems, it is unlikely that there is contact between the web and the roller over the entire surface. Thus, a real system would almost certainly resemble the second case. Unfortunately, this type of system is more difficult to model. Whether the web and roller are in contact at a point does not depend solely on the roughness magnitude there. It also depends on the magnitudes of the roughness of the points which are near that point.

This requires detailed knowledge of additional statistical characteristics of the surface roughness of the roller. Thus, an average model would not be applicable for the second case. However, it is possible to develop such a model for the more ideal conditions of the first case.

#### 4.3.1 Assumptions and Basic Equations

Three major assumptions are made in the development of the following model. First, as for the case of the grooved roller, the air film is able to distribute itself easily into the roughness valleys of the roller. In other words, the web will remain in contact with the roller at a point until the air film is large enough that every point lower than that point is no longer in contact with the web. Second, at points where the web and roller are not in contact, the web lies flat above the roller. The web does not follow the roller surface roughness except at points where the web and roller are in contact. Finally, it is assumed that the rough roller transports the same cross-sectional area of air in the constant gap region as a smooth roller operating at the same conditions.

To simplify the development of the model, only the constant gap region of the web/roller system will be considered. The web is assumed to be infinitely wide and perfectly flexible. Also, the roller roughness is such that the web is able to follow the surface of the roller closely. The web/roller system is operating at a certain set of conditions (velocity, tension, etc.). Figures 9a and 9b show sketches of a system with a smooth roller and a roughened roller operating at these conditions under current assumptions. The film height for the smooth roller is determined from Equation (1-5). For the case of perfect traction, this is:

$$h_0 = 0.643R \left( \frac{12\mu U}{T} \right)^{\frac{2}{3}} \quad (4-1)$$

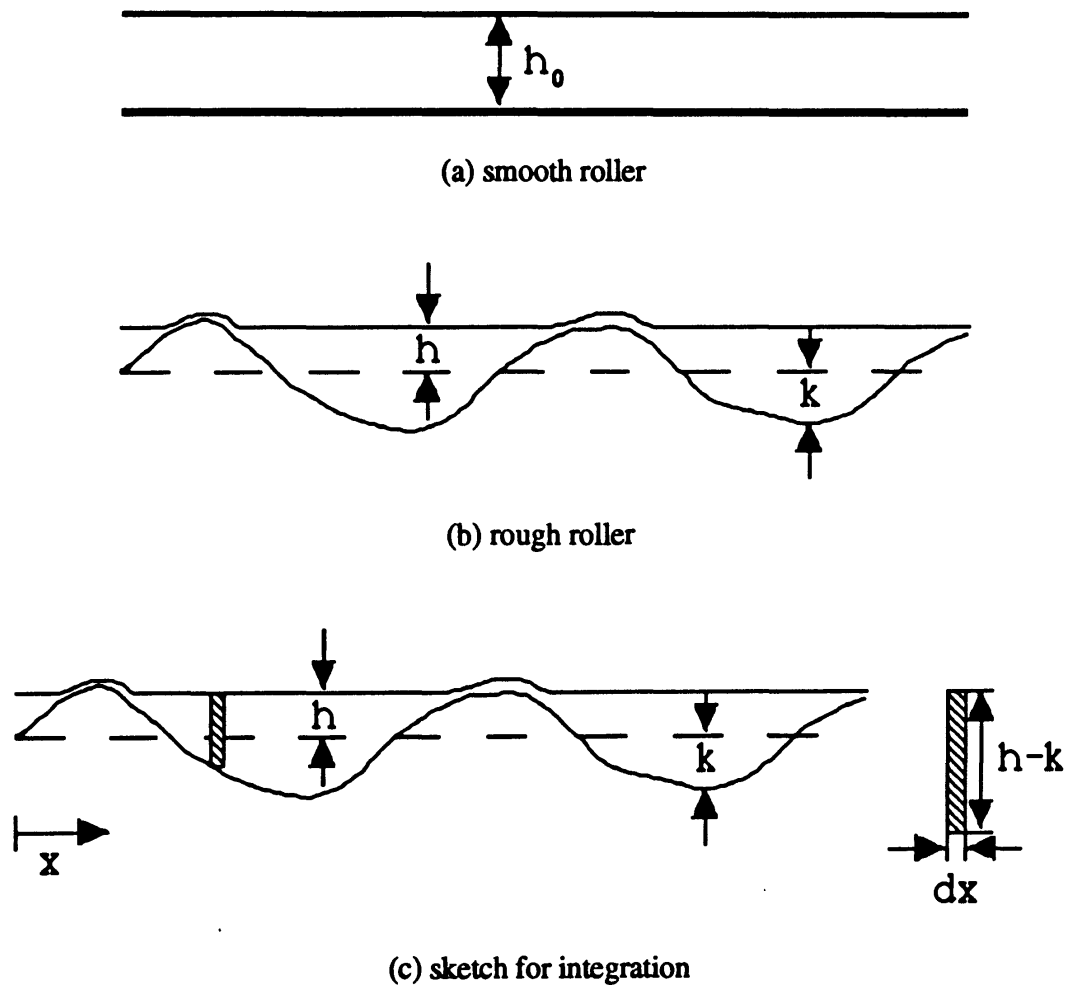


Figure 9. Transverse View of the Constant Gap Regions of a Smooth Roller and a Rough Roller Operating at the Same Conditions

The height of the web over the rough roller is measured from the reference point where the surface roughness of the roller has zero mean.

For a roller section of width  $w$ , the cross-sectional area between the web and the smooth roller is:

$$A_{\alpha} = h_0 w \quad (4-2)$$

The cross-sectional area for the rough roller is not as simple to determine. It is possible to integrate the area between the web and roller to obtain this area. Figure 9c is a sketch which helps to set up this integration. The variable  $k$  is the roller roughness height at a point and depends on  $y$ . The area between the web and roller is computed as the area between two curves. Thus,

$$A_{\alpha} = \int_x f(x) dx \quad (4-3)$$

where  $f(x)$  is the distance between the web and the roller. From Figure 9, it can be observed that:

$$\begin{aligned} f(x) &= h - k & , k \leq h \\ f(x) &= 0 & , k > h \end{aligned} \quad (4-4)$$

The integration could now be performed to find  $A_{\alpha}$ . However, detailed information about the roller roughness height ( $k$ ) is needed to perform this calculation. So, to find the height of the web above the roller without such information, a different approach must be used.



#### 4.3.2 Use of Probability to Determine the Average Height

As for the traction model, probability will be used to create a model for the average film height over a rough roller. However, in this case, the probability density function of the roller roughness is of interest. Assuming the roller has a roughness probability density function of  $p$ , then, by definition,  $p(k)$  is the probability that the roller roughness height is  $k$ . It is then assumed that the roller section of width  $w$  has the same roughness characteristics of the entire roller. As a result,  $p(k)$  is also the probability that the roller roughness height in the section is  $k$ . Or, more importantly, it is the fraction of the roller section which has a roughness height of  $k$ . Thus, by definition, the length of the portion of the roller with roughness height  $k$  in the section of width  $w$  is:

$$L(k) = p(k)w \quad (4-5)$$

The total cross-sectional area above the roughness of this height in the section would therefore be this length multiplied by the distance between the web and the roller for this value of  $k$ . So,

$$A_{\alpha}(k) = g(k)L(k) = g(k)p(k)w \quad (4-6)$$

To compute the total cross-sectional area between the web and the roller, the contribution from all possible values of  $k$  must be added together. This is done by integrating over all possible values of  $k$ .

$$A_{\alpha_t} = \int_k A_{\alpha}(k) dk = \int_k g(k)p(k)w dk = w \int_k g(k)p(k) dk \quad (4-7)$$

Since  $w$  is constant with respect to  $k$ , it was moved outside of the integral. Also, from previous examination of the system, it is known that;

$$\begin{aligned} g(k) &= h - k & , k \leq h \\ g(k) &= 0 & , k > h \end{aligned} \quad (4-8)$$

Studying Equation (4-8), it is noticed that there is no contribution to the integral for values of  $k$  larger than  $h$ . This reduces the integral to:

$$A_{\alpha_1} = w \int_{ksh} g(k)p(k) dk = w \int_{ksh} (h - k)p(k) dk \quad (4-9)$$

For the cross-sectional areas of the smooth and rough rollers to be equal, the following must be true.

$$w \int_{ksh} (h - k)p(k) dk = h_0 w \quad (4-10)$$

Substituting for  $h_0$  and dividing through by  $w$  yields:

$$\int_{ksh} (h - k)p(k) dk = h_0 \quad (4-11)$$

Equation (4-11) models the average air film height of a web over a rough roller in the constant gap region in terms of the roughness probability density function and the air film height of a smooth roller operating at the same conditions. Detailed knowledge of the roller roughness is not necessary. However, the roughness wavelength must be sufficiently large that the web can follow the roller roughness closely.

## CHAPTER V

### FORMULATION OF COMBINED MODELS FOR CALCULATIONS

#### 5.1 Introduction

In this section, the traction and grooving models are combined for computations which determine the amount of grooving necessary for a web/roller system to maintain perfect traction if certain system variables are changed. There are some general assumptions that are made for all of the following calculations. The first assumption is that the traction force necessary for perfect traction to exist between the web and the roller is not dependent on the characteristics of the system that are being varied. (For these calculations, the velocity and the tension are the characteristics changed.) It is constant for a particular web/roller system and only changes if the web and/or the rollers are changed. As a result, if perfect traction exists at a certain set of conditions which produces a given traction force, any set of conditions generating the same traction force is also presumed to have good traction. (Note: Good traction and perfect traction are used interchangeably.)

Further, the following calculations are based upon the assumption that, if the traction characteristics of two systems are the same in the constant gap region, they are the same everywhere. This assumption is reasonable if most of the traction for the web/roller system is generated in the constant gap region, which should be true for large wrap angles with sizable constant gap regions. However, for very small wrap angles, more traction could possibly be generated in the exit region where the film height is smaller. However, it will be assumed in such cases the traction increases proportionally everywhere the same as in the constant gap region.

## 5.2 First Grooving Approximation-Height Dependent Only

As a first approximation, it was assumed that whether or not a web/roller system had perfect traction was totally dependent on the film height above the roller. If perfect traction were present at a certain film height above the surface of the roller, then perfect traction would always exist if the web were at that height above the surface of the roller, regardless of the presence of grooving on the roller. This assumption is very limited since it does not take into account a traction model or the loss of traction due to the increased film height above the grooves of the roller.

### 5.2.1 Development of Equations

The approach for the calculations is as follows. Assume perfect traction exists for a certain web/roller system with velocity  $U_1$ , tension  $T_1$ , roller radius  $R_1$ , and viscosity  $\mu_1$ . If the roughness is assumed to have no effect on the air film height, the film height can be determined from Equation (1-5) for the smooth roller:

$$h_{0_1} = 0.643R_1 \left( \frac{12\mu U_1}{T_1} \right)^{\frac{2}{3}} \quad (5-1)$$

A sketch of the section of the web/roller system of width  $w$  appears in Figure 10a.

Now, assume the same web/roller system is operating at a different, higher velocity  $U_2$  with all other variables in the system remaining constant. Once again, from Equation (1-5), the film height of this system is (assuming perfect traction):

$$h_{0_2} = 0.643R_1 \left( \frac{12\mu U_2}{T_1} \right)^{\frac{2}{3}} \quad (5-2)$$

$$U_2 \geq U_1 \Rightarrow h_{0_2} \geq h_{0_1}$$

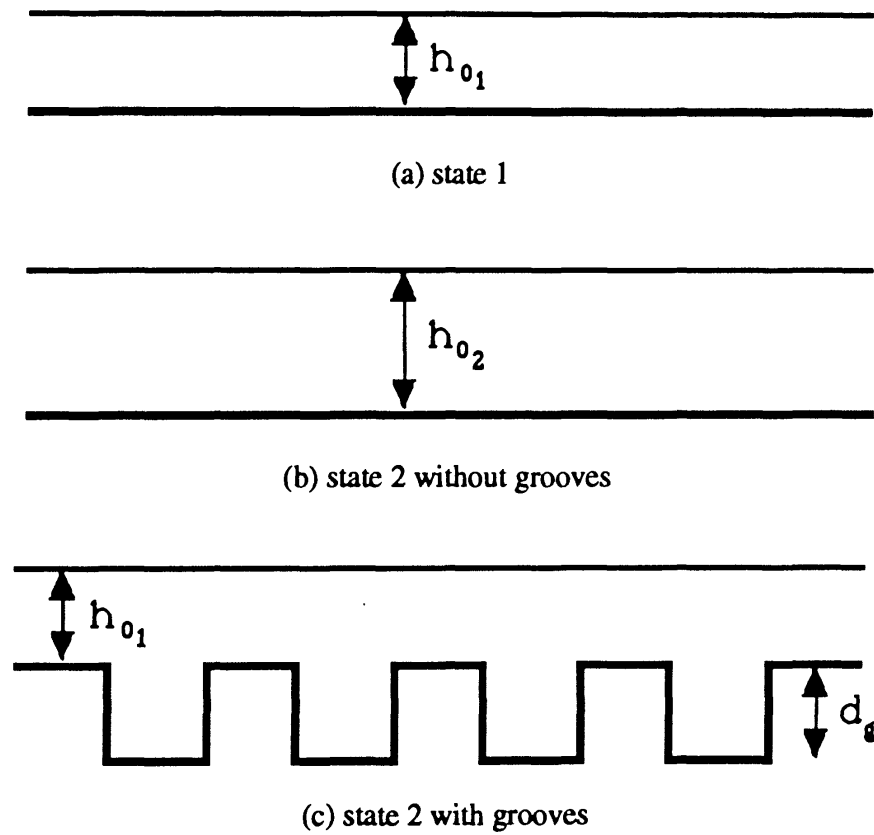


Figure 10. Transverse View of the Constant Gap Regions of Web/Roller System Operating at Two Different States

The sketch of the section of width  $w$  of the web/roller system at these conditions is shown in Figure 10b. It is unknown whether there exists good traction at this second state. However, it is known that the first state has good traction. Therefore, to assure the second state has good traction as well, grooves are added to the roller such that the film height over the surface for the second state is the same as for the first state so that the two states generate the same traction force. The second system now is shown in Figure 10c. All grooves are of uniform depth.

It is now necessary to determine the value for the groove fraction which produces a height above the surface of the roller for state 2 of  $h_{0_1}$ . Using Equation (3-13) and substituting  $h_{0_1}$  for  $h$  and  $h_{0_2}$  for  $h_0$  yields the following.

$$h_{0_1} = h_{0_2} - f_g d_g \quad (5-3)$$

The next step is to solve Equation (5-3) for  $f_g$ .

$$f_g d_g = h_{0_2} - h_{0_1}$$

$$f_g = \frac{h_{0_2} - h_{0_1}}{d_g} \quad (5-4)$$

Factoring out  $h_{0_1}$  gives the nondimensional form:

$$f_g = \frac{\left(\frac{h_{0_2}}{h_{0_1}}\right) - 1}{\left(\frac{d_g}{h_{0_1}}\right)} \quad (5-5)$$

Finally, substituting for the height from the foil bearing equation and simplifying give the final form:

$$f_g = \frac{\left(\frac{U_2}{U_1}\right)^{\frac{2}{3}} - 1}{\left(\frac{d_g}{h_{01}}\right)} \quad (5-6)$$

### 5.2.2 Calculations and Results

Equation (5-6) was used to generate plots of groove fraction versus the ratio of the final to the starting velocity. A simple computer program (see Appendix A) was written for the calculations. The film height ratio was varied from 1 to 5, and the ratio of both the groove depth and initial film height to roller radius were varied. Figure 11 is a graph of the results. It shows plots of groove fraction versus velocity ratio for different ratios of groove depth to initial film height. The velocity ratio is determined from the film height ratio and the air film height equation for a smooth roller. As expected, the groove fraction increases as the velocity ratio increases for all cases. Also, as can be seen, larger ratios of groove depth to initial film height lead to smaller groove fractions. This makes sense physically since deeper grooves can transport more air per unit width than shallower ones. Thus, less grooving is needed.

### 5.3 Second Grooving Approximation-Linear Probability Distribution

The first grooving approximation, while very simple to compute, only gives a rough estimate of the amount of grooving that may be necessary for the two states to have the same traction characteristics. To have more accurate results, it is necessary to have a better traction model for the system. In particular, one should account for the loss

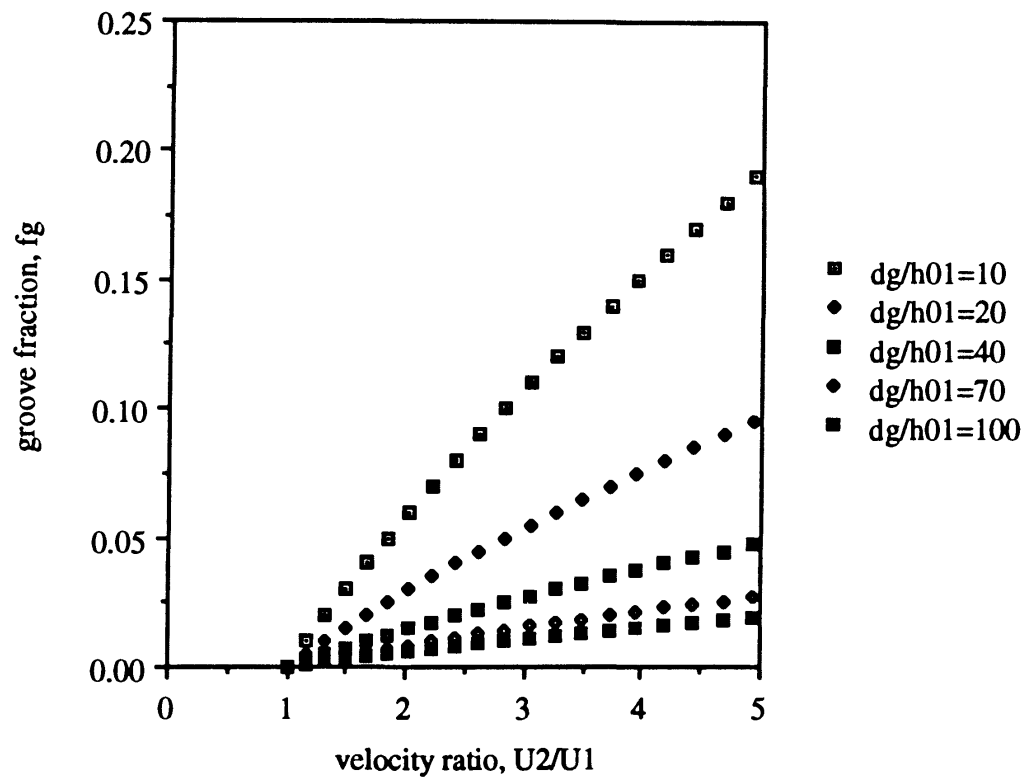


Figure 11. Groove Fraction versus Velocity Ratio for Various Ratios of Groove Depth to Initial Film Height for the Height Dependent Model



of traction above the grooves. In order to do this, the traction model developed earlier will be used.

A very simple model is to assume that the traction increase is directly proportional to the decrease in film height. Thus, the probability distribution in Equation (2-13) would be linear in nature.

$$\begin{aligned}
 P(k) &= 0 & , k < 0 \\
 P(k) &= \frac{k}{h^*} & , 0 \leq k \leq h^* \\
 P(k) &= 1 & , k > h^*
 \end{aligned}
 \tag{5-7}$$

where  $h$  is the film height and  $h^*$  is the film height at which traction between the web and roller reaches zero. Using the same assumptions as the first grooving approximation, similar calculations can be performed.

### 5.3.1 Development of Equations

Once again, the system starts at a state 1 with certain velocity, tension, and other parameters. Good traction exists at state 1. The velocity is then increased to  $U_2$  while holding all other parameters constant. (Refer to sketches 12a and 12b, which are identical to 10a and 10b from the previous section). Grooves are once again added to the roller when the system is at state 2. Figure 10c is a sketch of the system at state 2 with the grooved roller. The sketch is the same as for the previous calculation except that the height of the web over the surface is  $h_2$  instead of  $h_{o_1}$ .

It is desired to groove the roller such that the second state has the same traction characteristics as the first state. However, the height  $h_2$  must be known before any traction calculations can be made for the grooved roller. The height calculations are performed

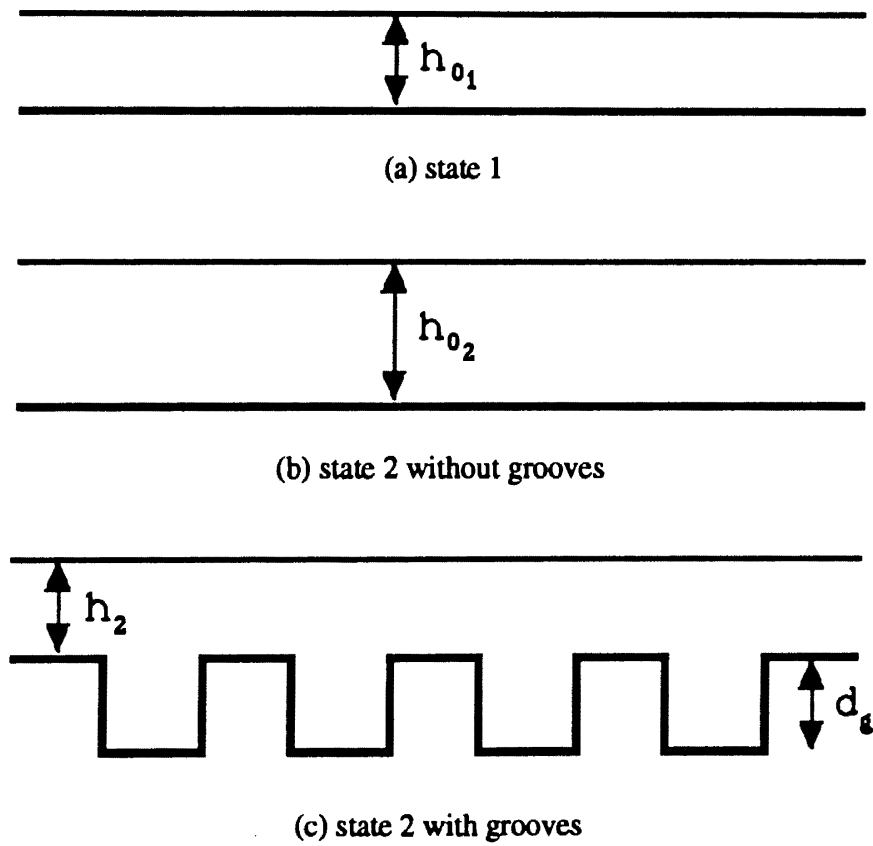


Figure 12. Transverse View of the Constant Gap Regions of a Web/Roller System Operating at Two Different States

using the grooving approximation. Thus, using the Equation (3-13) and substituting  $h_{0_2}$  for  $h_0$  and  $h_2$  for  $h$ , it can be determined that:

$$h_2 = h_{0_2} - f_g d_g \quad (5-8)$$

This is the height of the web above the surface at state 2 after the addition of grooves.

Now, for the traction characteristics at the two states to be the same, the states must generate the same traction force. For the roller section of width  $w$ , the traction force at state one per unit length along the roller is determined from Equation (2-13) by substituting  $h_{0_1}$  for  $h$  and  $w$  for the integral and by using the linear probability distribution in Equation (5-7). The result is:

$$\overline{F}_{f_{t_1}} = wL\mu_s \frac{T}{R} \left[ 1 - \left( \frac{h_{0_1}}{h^*} \right) \right] \quad (5-9)$$

Once again, the traction force at state two has to be computed in two parts. The traction force at state 2 above the surface of the roller per unit length, which is figured by substituting  $h_2$  into the equation and multiplying by the length of the surface in the section  $((1 - f_g)w)$ , is therefore:

$$\overline{F}_{f_{t_2s}} = (1 - f_g)wL\mu_s \frac{T}{R} \left[ 1 - \left( \frac{h_2}{h^*} \right) \right] \quad (5-10)$$

The traction force at state 2 above the grooves per unit length, with a film height of  $h_2 + d_g$  and a length of  $f_g w$ , would then be:

$$\overline{F}_{f_{t_2g}} = f_g wL\mu_s \frac{T}{R} \left[ 1 - \left( \frac{h_2 + d_g}{h^*} \right) \right] \quad (5-11)$$

Thus, the total traction force at state two would be the sum of these two parts, or:

$$\overline{F}_{f_{t_2}} = \overline{F}_{f_{t_{2s}}} + \overline{F}_{f_{t_{2g}}} = (1 - f_g)wL\mu_s \frac{T}{R} \left[1 - \left(\frac{h_2}{h^*}\right)\right] + f_g wL\mu_s \frac{T}{R} \left[1 - \left(\frac{h_2 + d_g}{h^*}\right)\right] \quad (5-12)$$

However, it will be assumed that  $d_g > h^*$ . Thus, the traction force of the section above the grooves would be zero, leaving:

$$\overline{F}_{f_{t_2}} = (1 - f_g)wL\mu_s \frac{T}{R} \left[1 - \left(\frac{h_2}{h^*}\right)\right] \quad (5-13)$$

So, if the traction forces generated by the two states are equal, this implies:

$$wL\mu_s \frac{T}{R} \left[1 - \left(\frac{h_{01}}{h^*}\right)\right] = (1 - f_g)wL\mu_s \frac{T}{R} \left[1 - \left(\frac{h_2}{h^*}\right)\right] \quad (5-14)$$

Factoring out the common terms leaves:

$$\left[1 - \left(\frac{h_{01}}{h^*}\right)\right] = (1 - f_g) \left[1 - \left(\frac{h_2}{h^*}\right)\right] \quad (5-15)$$

Substituting for  $h_2$  gives:

$$\left[1 - \left(\frac{h_{01}}{h^*}\right)\right] = (1 - f_g) \left[1 - \left(\frac{h_{02} - f_g d_g}{h^*}\right)\right] \quad (5-16)$$

Expanding all the terms:

$$1 - \left(\frac{h_{01}}{h^*}\right) = 1 - f_g - \left(\frac{h_{02}}{h^*}\right) + f_g \left(\frac{d_g}{h^*}\right) + f_g \left(\frac{h_{02}}{h^*}\right) - f_g^2 \left(\frac{d_g}{h^*}\right) \quad (5-17)$$

Rearranging:

$$\left(\frac{d_g}{h^*}\right)f_g^2 + \left[1 - \left(\frac{d_g}{h^*}\right) - \left(\frac{h_{02}}{h^*}\right)\right]f_g + \left[\left(\frac{h_{02}}{h^*}\right) - \left(\frac{h_{01}}{h^*}\right)\right] = 0 \quad (5-18)$$

Using the quadratic formula to solve for  $f_g$  yields:

$$f_g = \frac{-\left[1 - \left(\frac{d_g}{h^*}\right) - \left(\frac{h_{02}}{h^*}\right)\right] \pm \sqrt{\left[1 - \left(\frac{d_g}{h^*}\right) - \left(\frac{h_{02}}{h^*}\right)\right]^2 - 4\left(\frac{d_g}{h^*}\right)\left[\left(\frac{h_{02}}{h^*}\right) - \left(\frac{h_{01}}{h^*}\right)\right]}}{2\left(\frac{d_g}{h^*}\right)} \quad (5-19)$$

taking only the solution which gives a groove fraction between 0 and 0.5.

### 5.3.2 Calculations and Results

A computer program was written to solve Equation (5-19). In the program, the film height ratio was varied from 1 to 5, and the groove depth to initial film height was varied from 10 to 100. The ratio of  $h_{01}$  to  $h^*$  was assumed to be 0.5 for the calculations.

A plot of the results can be seen in Figure 13. The graph shows plots of groove fraction versus velocity ratio for different groove depth to initial film height ratios. The velocity ratio is determined in the same manner as the first grooving approximation. Once again, the film height increases as the velocity ratio increases. Also, larger groove depth to initial film height ratios produce smaller groove fractions. Both of these results are consistent with those of the previous approximation and with expectations.

## 5.4 Third Grooving Approximation-Gaussian

### Probability Distribution

While the linear probability distribution is simple to compute, it is seldom applicable to real world situations. Thus, it is desirable to find solutions for other probability

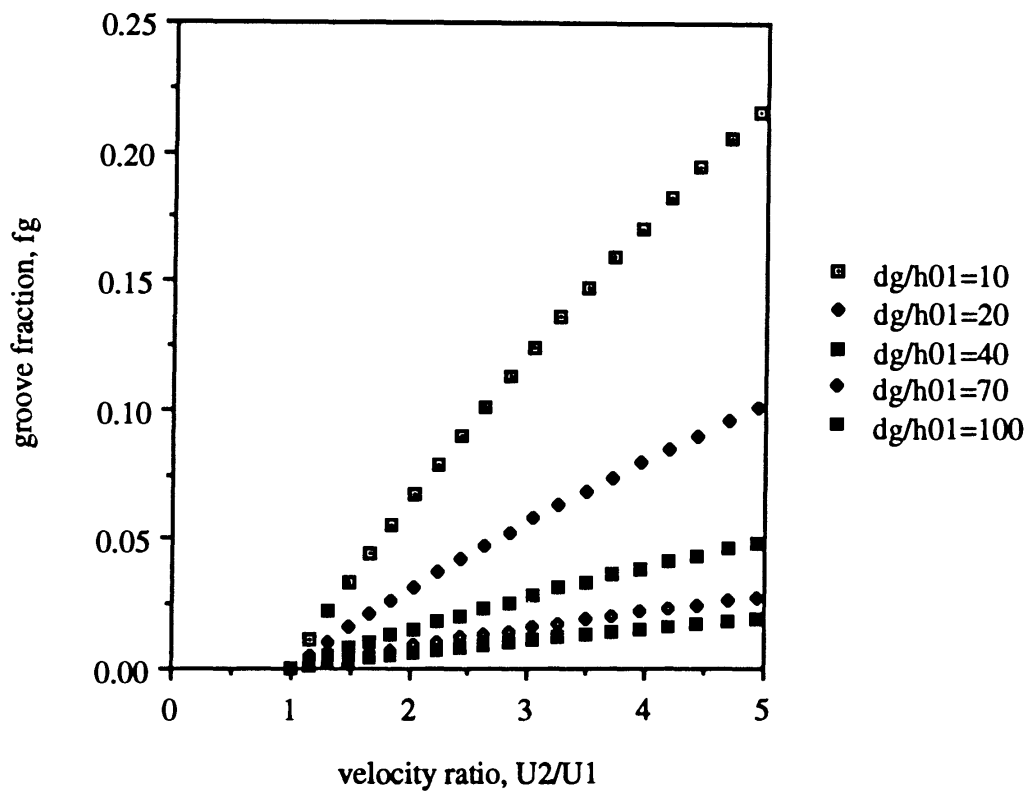


Figure 13. Groove Fraction versus Velocity Ratio for Various Ratios of Groove Depth to Initial Film Height for the Linear Probability Distribution

distributions. The Gaussian distribution is of particular interest since it is often used to model a random roughness distribution. To provide a solution for the Gaussian distribution, a solution for the combined traction and grooving models will be found for a general probability distribution.

#### 5.4.1 Development of Solution for a Generalized Probability Distribution

Once again, a certain web/roller system operates at certain conditions called state 1 (with a velocity of  $U_1$ , etc.). The film height at these conditions is  $h_{o_1}$  and is determined from the foil bearing equation. Refer to Figure 12a for a sketch of the system.

The traction force between the web and the roller at this state for a section of the web/roller system of width  $w$  is determined by equation (2-13). After evaluating the integral, the result is:

$$\overline{F}_{r_{t_1}} = \mu_s L w \{1 - P(h_{o_1})\} \frac{T}{R} \quad (5-20)$$

The web/roller system at state 1 is assumed to have good traction (i.e., no slip between the web and roller).

Now, assume that the same web/roller system operates at a different state 2. All variables in this system are unchanged from those in state one except that the velocity is increased to  $U_2$ . This greater velocity leads to a larger film height  $h_{o_2}$  (refer to Figure 12b). It is unknown if the traction force at this state is sufficient for no slip between the web and roller. However, grooves can be added to the roller so that the state will generate the same average traction force as state 1. Refer to Figure 12c for a sketch of state 2 with grooves added to the roller.

The first step in equating the traction forces generated by the two states is determining  $h_2$ . The inclusion of roughness would make this slightly more complex, but it will be assumed (as it was for the film heights at state 1 and state 2 without grooving)

that  $h_2$  is sufficiently large that the effects on air transport from the roughness peaks and valleys can be ignored. As a result, the value of  $h_2$  will be the same as that computed from the second grooving approximation. Thus,

$$h_2 = h_{0_2} - f_g d_g \quad (5-21)$$

Next, the traction force generated by the grooved roller at state 2 must be computed. This is the same as the computations made for the second grooving approximation. Thus, the traction force generated by the portion of the web above the surface of the roller (in the section of width  $w$ ) is,

$$\overline{F_{f_{t_2s}}} = (1 - f_g) \mu_s L w \{1 - P(h_2)\} \frac{T}{R} \quad (5-22)$$

Similarly, the traction force generated by the portion of the web above the grooves is:

$$\overline{F_{f_{t_2g}}} = f_g \mu_s L w \{1 - P(h_2 + d_g)\} \frac{T}{R} \quad (5-23)$$

However, as for the second approximation, it is assumed that the groove depth is large enough that the traction contribution from the sections where the web is above the grooves is negligible. Thus,

$$\overline{F_{f_{t_2}}} = \overline{F_{f_{t_2s}}} = (1 - f_g) \mu_s L w \{1 - P(h_2)\} \frac{T}{R} \quad (5-24)$$

Equating the traction force at the two states yields,

$$(1 - f_g) \mu_s L w \{1 - P(h_2)\} \frac{T}{R} = \mu_s L w \{1 - P(h_{0_1})\} \frac{T}{R} \quad (5-25)$$



Dividing out all common terms leaves

$$(1 - f_g)(1 - P(h_2)) = \{1 - P(h_{0_1})\} \quad (5-26)$$

Substituting for  $h_2$  gives the final form:

$$(1 - f_g)\{1 - P(h_{0_2} - f_g d_g)\} = \{1 - P(h_{0_1})\} \quad (5-27)$$

#### 5.4.2 Calculations and Results for the Gaussian Roughness Distribution

With knowledge of the roughness probability distribution function, calculations similar to those in the first two grooving approximations may be made. Now, however, any distribution can be used. The Gaussian distribution is one that is of particular interest. Calculations were made using a Gaussian distribution for the roughness heights. The ratio of the film height at state 1 to the roughness rms was assumed to be 3 since Patir and Cheng (1978) say that, at that point, the partial lubrication regime begins and there is significant asperity contact between the two surfaces. A computer program was written to solve Equation (5-27) iteratively for the groove fraction, varying the film height ratio and the groove depth to initial film height ratio. Plots of groove fraction versus the velocity ratio were made for different ratios of film height at state 1 to groove depth. The velocity ratio is computed as for the first two approximations. The results are shown in Figure 14.

As expected, the groove fraction increases as the velocity ratio increases. Also, larger groove depth to initial height ratios yield smaller groove fractions. The results are similar to those obtained by the first two grooving approximations. Thus, a comparison between the results from the three grooving approximations is of interest. Figure 15

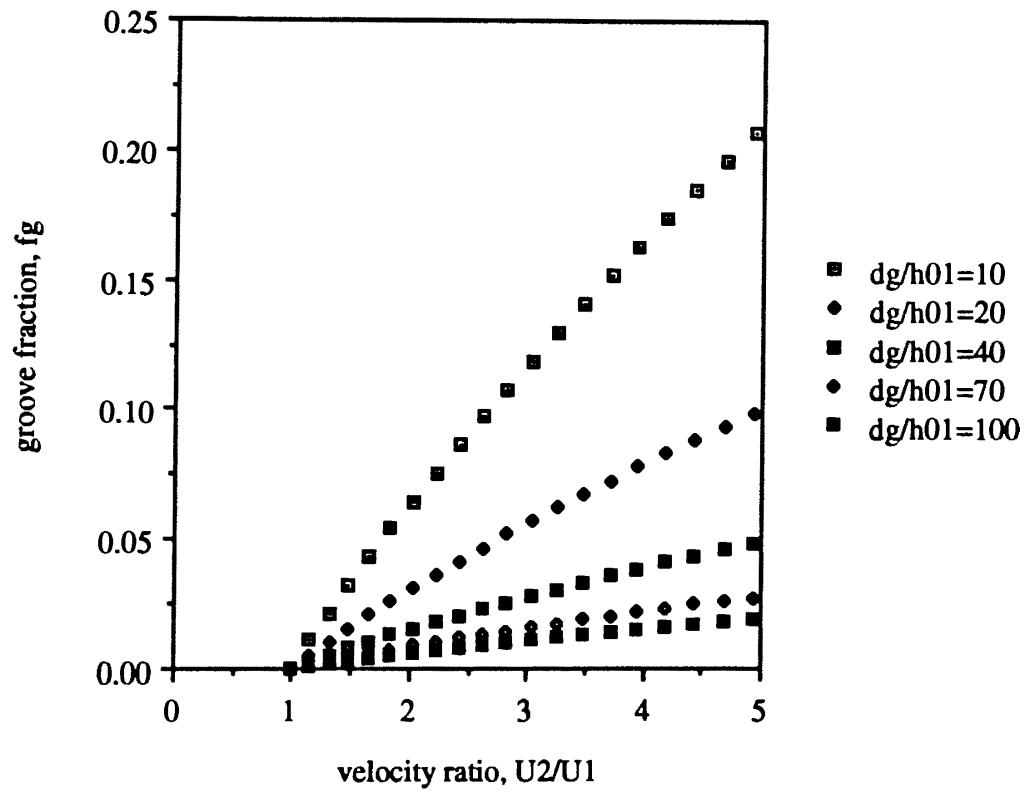


Figure 14. Groove Fraction versus Velocity Ratio for Various Ratios of Groove Depth to Initial Film Height for the Gaussian Probability Distribution

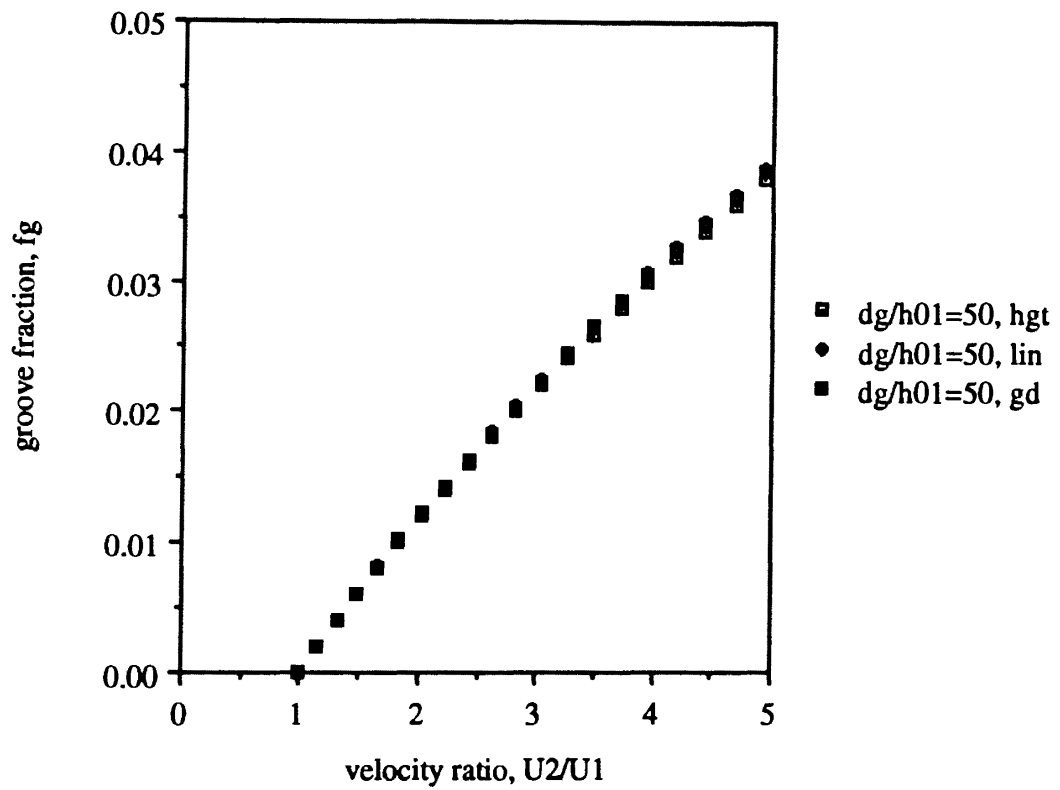


Figure 15. Groove Fraction versus Velocity Ratio for a Groove Depth to Initial Film Height Ratio of 50 for the Three Previous Models

shows plots of the data generated by the three approximations for a groove depth to initial film height ratio of 50.

Observing the figure, there appears to be little difference between the three approximations for this case. To discover if the changes are dependent on the groove depth to initial film height ratio, plots of the percent change in groove fraction from one approximation to another will be made for different values of this ratio. Figure 16 compares the first and second approximation, and Figure 17 compares the first and third approximation.

The Figures show that the fractional change in the results of the three approximations is not very large. It appears to slightly increase as the velocity ratio increases, except for a few points at the low end of the Gaussian-height comparison. This is due to lower accuracy of the groove fraction for the Gaussian distribution at low velocity ratios. The fractional change decreases as the groove depth to initial film height ratio increases, but it is always small (never exceeding 0.15). This was unexpected since both the second and third approximations take into account the reduction of surface due to the grooves on the roller while the first approximation does not. However, a closer examination of the grooving approximation shows the reason for these small differences.

First, assume that there is a grooved roller which follows the grooving approximation. The film height over the surface of the roller is given by Equation (3-13).

$$h = h_0 - f_g d_g \quad (5-28)$$

Now, assume some incremental change in the groove fraction,  $\Delta f_g$ . This small change in groove fraction causes a small change in height,  $\Delta h$ . Substituting  $f_g + \Delta f_g$  for  $f_g$  and  $h + \Delta h$  for  $h$  in Equation (3-13) yields:

$$h + \Delta h = h_0 - (f_g + \Delta f_g) d_g \quad (5-29)$$

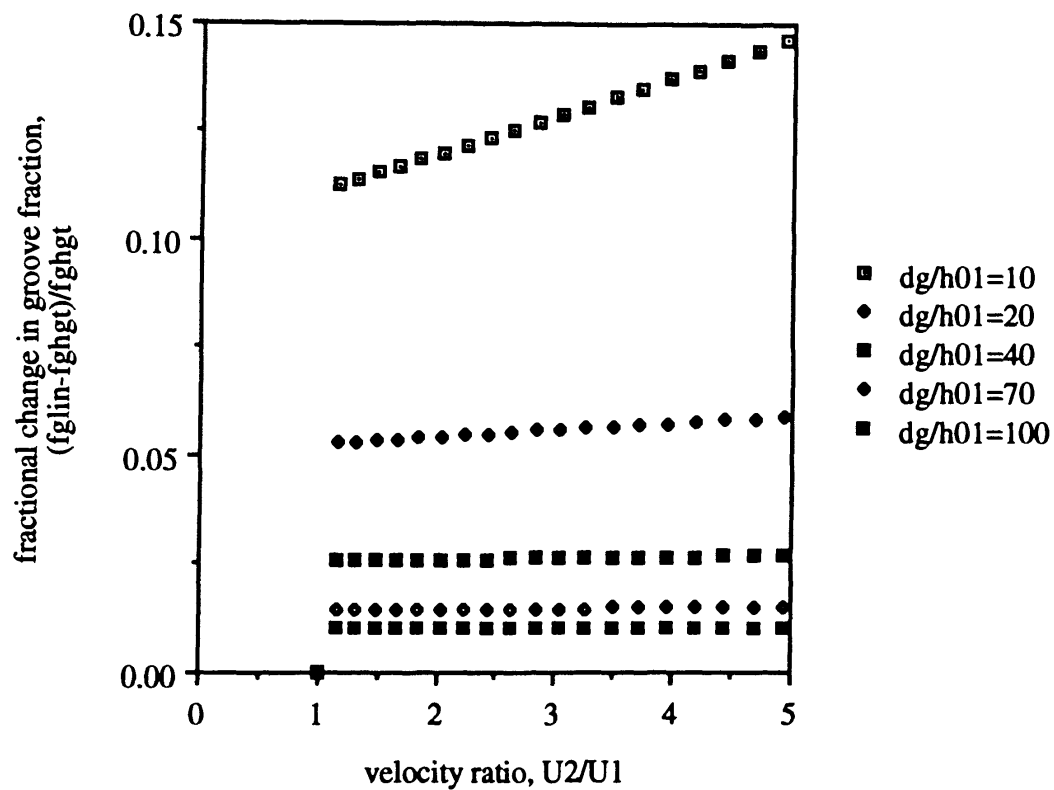


Figure 16. The Fractional Change in Groove Fraction from the Height Dependent Model to the Linear Probability Distribution versus Velocity Ratio for Various Ratios of Groove Depth to Initial Film Height

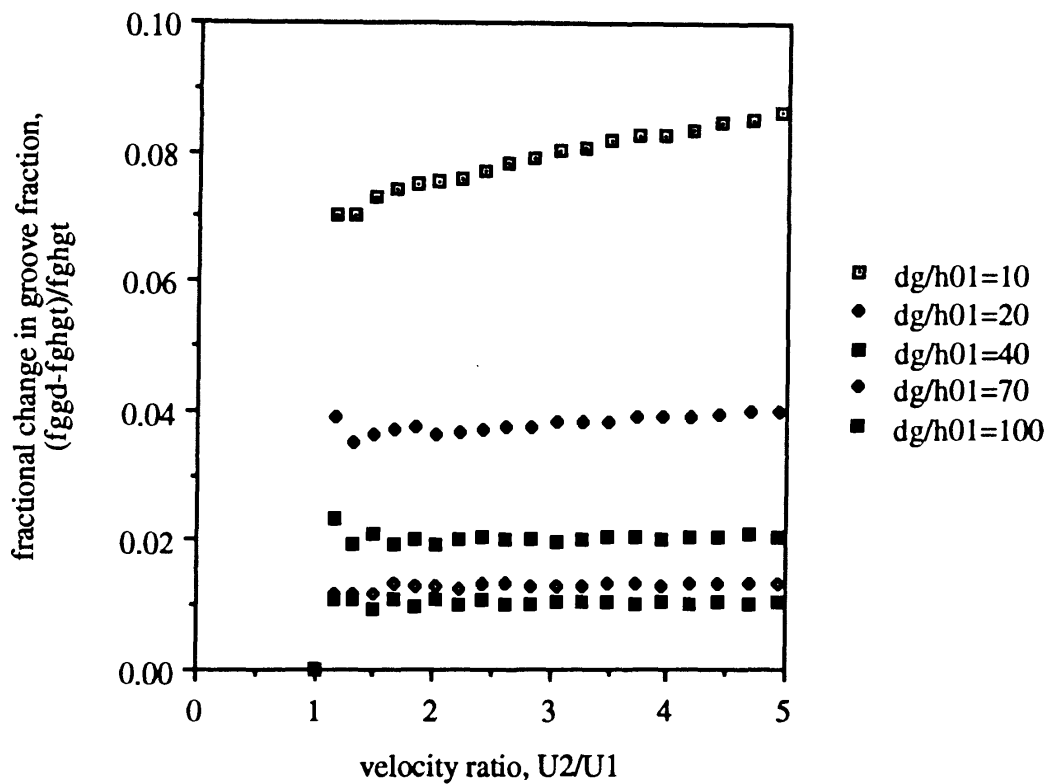


Figure 17. The Fractional Change in Groove Fraction from the Height Dependent Model to the Gaussian Probability Distribution versus Velocity Ratio for Various Ratios of Groove Depth to Initial Film Height

Expanding all the terms:

$$h + \Delta h = h_0 - f_g d_g - \Delta f_g d_g \quad (5-30)$$

Removing the relationship in Equation (5-28) yields:

$$\Delta h = -\Delta f_g d_g \quad (5-31)$$

Dividing both sides through by  $h$  yields:

$$\frac{\Delta h}{h} = -\Delta f_g \frac{d_g}{h} \quad (5-32)$$

For the calculations above,  $\frac{d_g}{h_0}$  is a minimum of 10. This means that a 1% change in groove fraction causes a 10% change in film height. For this reason, the values calculated by the three approximations are relatively close.

## 5.5 Fourth Grooving Approximation-Tension Variation

All of the previous calculations have been based on changes in velocity while holding all other variables constant. The traction force model allows variations of other parameters as well. Most notably, tension could be the parameter changed. This has a dual effect on the system since the tension appears both in the traction force and the film height equations. This modifies the solution slightly.

### 5.5.1 Development of Equations

As before, there exists a state 1 at certain conditions ( $U_1$ ,  $T_1$ , etc). The film height at this state for perfect traction is determined from Equation 1-5.

$$h_{0_1} = 0.643R_1 \left( \frac{12\mu U_1}{T_1} \right)^{\frac{2}{3}} \quad (5-33)$$

Refer to Figure 12a for a sketch of this system. The web/roller system at this state has perfect traction. The system is then brought to state 2 by decreasing the tension and holding all other variables constant. The film height for this state (if perfect traction exists) would be:

$$h_{0_2} = 0.643R_1 \left( \frac{12\mu U_1}{T_2} \right)^{\frac{2}{3}} \quad (5-34)$$

Refer to Figure 12b for a sketch of this state. It is unknown whether state 2 has good traction, so grooves are added to the roller so that state 2 will generate the same average traction force as state 1 (refer to Figure 12c). From previous analysis, it is known that the relationship between  $h_2$  and  $h_{0_2}$  is described by Equation (3-13).

$$h_2 = h_{0_2} - f_g d_g \quad (5-35)$$

The derivation is very similar to the one for a general probability distribution except that the tensions for both states differ. Thus, the average traction force generated by state 1 for a roller section of width  $w$  is:

$$\overline{F_{t_1}} = \mu_s L w \{1 - P(h_{0_1})\} \frac{T_1}{R_1} \quad (5-36)$$

The average traction force generated above the surface of the roller at state 2 would then be:

$$\overline{F_{t_2}} = (1 - f_g) \mu_s L w \{1 - P(h_2)\} \frac{T_2}{R_1} \quad (5-37)$$



Once again, the average traction force generated above the grooves of the roller will be neglected. Thus, the average traction force generated by state 2 is:

$$\overline{F}_{t_2} = \overline{F}_{t_{2a}} = (1 - f_g)\mu_s Lw\{1 - P(h_2)\} \frac{T_2}{R_1} \quad (5-38)$$

Equating the average traction forces from state 1 and state 2 yields:

$$(1 - f_g)\mu_s Lw\{1 - P(h_2)\} \frac{T_2}{R_1} = \mu_s Lw\{1 - P(h_{0_1})\} \frac{T_1}{R_1} \quad (5-39)$$

Dividing out all the common terms and substituting for  $h_2$  leaves the final form:

$$(1 - f_g)\{1 - P(h_{0_2} - f_g d_g)\} T_2 = \{1 - P(h_{0_1})\} T_1 \quad (5-40)$$

### 5.5.2 Calculations and Results

A computer program was written to solve Equation (5-40) iteratively for groove fraction for values of the ratio of initial tension to final tension ranging from 1 to 2.5 using the Gaussian probability distribution. The groove depth to initial film height ratio was varied from 10 to 100. Plots were made of the groove fraction versus the tension ratio for the different ratios of groove depth to initial film height. Figure 18 is a graph of the results.

From the graph, it can be observed that, as the tension ratio increases (the tension at state 2 becomes smaller with respect to the tension at state 1), the necessary groove fraction increases. Also, the groove fraction increases more quickly compared to that of the Gaussian distribution in which the velocity ratio is the parameter varied. This agrees with expectations since a reduction in tension not only increases the film height, but also decreases the normal force between the web and the roller. Also, as previously found for

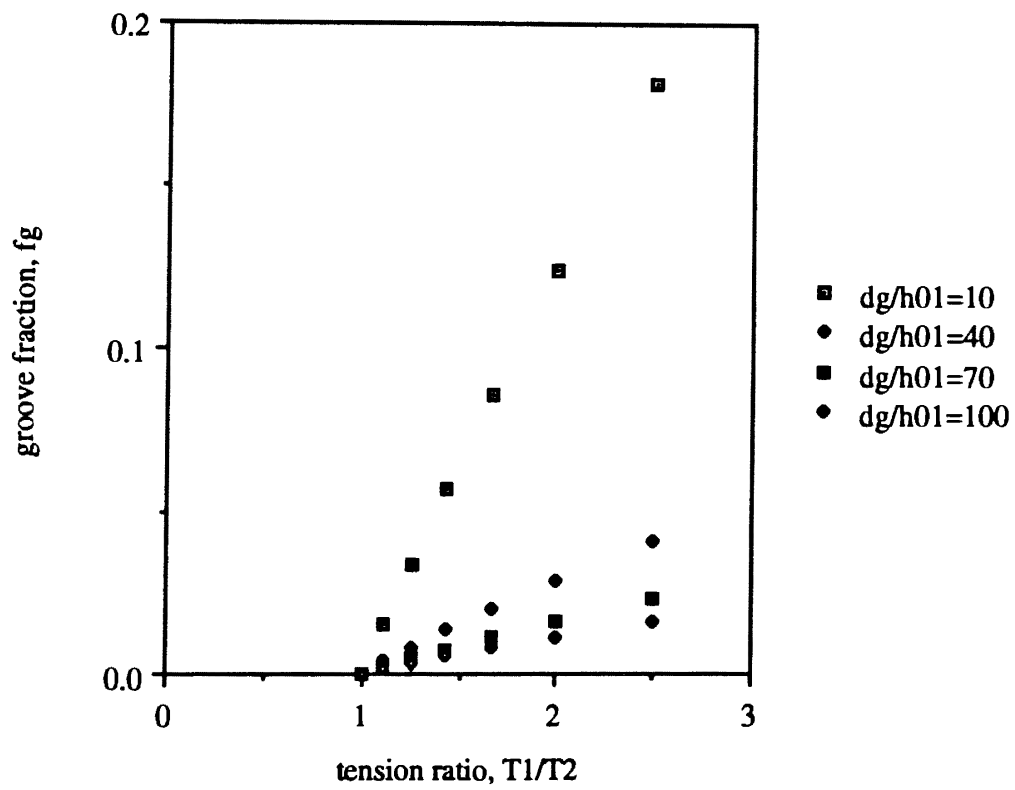


Figure 18. Groove Fraction versus Tension Ratio for Various Ratios of Groove Depth to Initial Film Height for the Gaussian Probability Distribution

the other calculations, the necessary groove fraction decreases as the groove depth to initial film height ratio increases.

## 5.6 Summary

The above sections use the previously developed models for traction and grooving to generate curves of conditions that produce a constant traction force. The first three changed the groove fraction of the web/roller system to account for a change in velocity, and the final one changed the groove fraction to account for a change in the tension. The difference in the first three is in the choice of traction condition or probability distribution.

For all three traction conditions or probability distributions used for the calculation of groove fraction due to a change in velocity, the groove fraction increased as the velocity ratio of state 2 to state 1 increased. This result agreed with expectations and observations in industry that more grooving is needed to keep good traction in a system as the velocity is increased. Further, the two probability distributions produced slightly higher groove fractions than the height dependent traction model. This also agreed with expectations since the probability distribution models took into account the loss of traction due to the increased film height over the grooves while the height dependent model did not.

For the calculation of groove fraction due to a change in tension, the groove fraction increased as the tension ratio of state 1 to state 2 increased. Further, this increase in groove fraction occurred more quickly than that of the velocity ratio. This result agreed with expectations since the reduction in tension not only increased the film height but also decreased the normal force between the web and the roller.

For ease of use, the height dependent model is the simplest to calculate and, at large groove depth to initial film height ratios, is nearly as accurate as the probability-based traction model. However, the assumptions used for the height dependent model only allow its use for a system in which the velocity is the parameter changed. The probability-based traction model allows other system parameters to be varied. It is important to note that, for

all the models, it is not necessary to know if good traction exists at any condition producing less traction than the initial state since all calculations are based on the traction at the chosen state. Thus, if any state can be found that has perfect traction (i.e., movement without slip), it can be used as the reference state for the calculations. As a result, the models presented give an upper bound on the necessary groove fraction if the assumptions used in their development hold. The linear probability distribution is the most conservative model for traction, predicting the largest groove fraction, and is still relatively easy to use since the groove fraction can be solved for explicitly, but the Gaussian probability distribution is often used to model random roughness and, with the lower groove fraction, would be less likely to cause web abrasion. So, all of the models have certain strengths and weaknesses.

The accuracy of the models is limited by the accuracy of the assumptions and approximations made in developing the models. It is assumed that the web lies flat above the grooved roller, but observations in wear patterns of grooved rollers show that the rollers tend to have more wear at the edges of the grooves than elsewhere. This supports the idea that the web tends to dip into the grooves rather than lie flat above them. Also, it is assumed for the calculations that the film height above the zero mean point of the roughness distribution of a rough roller is the same as that of a smooth roller operating at the same conditions. While this may be a good approximation at large film heights where the web and roller are only in contact at the largest asperities, it is not accurate at small film heights whether or not the web can follow the surface roughness of the roller closely. If the web follows the roughness closely, the roughness valleys transport all of the entrained air, producing a film height that is less than zero. If the web and roller are only in contact at the asperities, the web will have a nonzero film height with no entrained air. It is also unknown whether smooth rollers, rough rollers, and grooved rollers operating at the same conditions transport the same amount of air (especially the same cross-section of air). The validity of this assumption is very critical in the calculations. The effects of these and other factors on the traction in a web/roller system are unknown, but they should not be ignored.

## CHAPTER VI

### CONCLUSIONS

#### 6.1 Conclusions

Models have been developed to account for the effects of roughness and grooving on the traction and air film height of a web/roller system. The probability-based traction model and the grooving model were combined to perform calculations of the groove fraction necessary to have a web/roller system operating at two different conditions create the same traction force. These calculations were performed for various roughness distributions or traction assumptions. It was found that:

1. The groove fraction increased as the ratio of final to initial velocity increased. More grooving was necessary to transport the larger amount of air entrained as the velocity increased.
2. The groove fraction increased as the ratio of initial to final tension increased. This increase occurred more quickly than that of the velocity ratio since the lower final tension not only increased the film height but also decreased the normal force causing traction between the surfaces.
3. The groove fraction decreased as the ratio of the groove depth to the initial film height increased. This occurred because the deeper grooves could transport more air than the shallower ones.

These results held true for all the roughness distributions or traction conditions for which the computations were performed and agree with expectations.

It is important to note that this model is based on theory. As yet, no experimental data has been obtained to check the correlation of the predicted values to empirical results.

Further, the validity of the simplifying assumptions used for the calculations must be checked. A refinement of these assumptions should improve the accuracy of the model's predictions. This model could be useful in further web handling research, so its accuracy must be determined.

## 6.2 Suggestions for Further Research

The results presented here are for a very idealistic system. Through less restrictive assumptions, the traction model could be extended to a more realistic case. The following are some suggestions for further research into this area of web handling:

1. Traction calculations made for different height profiles of the web above the grooved roller (not just a flat web).
2. Integration of the average height model with the traction and grooving models for calculations.
3. Investigation into the ability of the entrained air to distribute itself into the grooves (e.g. determining the amount of side flow into the grooves, determining the time scale for flow into the grooves, etc.).
4. Expansion of the traction model to include effects of web flexibility.
5. Investigation into the effects of slip between the web and roller on traction between the surfaces.

## REFERENCES

- Barlow, E. J. (1967a). Derivation of Governing Equations for Self-Acting Foil Bearings. Transactions of the ASME: Journal of Lubrication Technology, 89, 334-340.
- Barlow, E. J. (1967b). Self-Acting Foil Bearings of Infinite Width. Transactions of the ASME: Journal of Lubrication Technology, 89, 341-345.
- Baumeister, H. K. (1963). Nominal Clearance of the Foil Bearing. IBM Journal of Research and Development, 7, 153-154.
- Bhushan, B., Sharma, B., & Bradshaw, R. (1984a). Friction in Magnetic Tapes I: Assessment of Relevant Theory. ASLE Transactions, 27, 33-44.
- Bhushan, B., Sharma, B., & Bradshaw, R. (1984b). Friction in Magnetic Tapes II: Role of Physical Properties. ASLE Transactions, 27, 89-100.
- Bhushan, B. (1984). Analysis of the Real Area of Contact Between a Polymeric Magnetic Medium and a Rigid Substrate. Transactions of the ASME: Journal of Tribology, 106, 26-34.
- Chang, L., & Webster, M. N. (1991). A Study of Elastohydrodynamic Lubrication of Rough Surfaces. Transactions of the ASME: Journal of Tribology, 113, 110-115.
- Chengwei, W., & Linqing, Z. (1989). An Average Reynolds Equation for Partial Film Lubrication with a Contact Factor. Transactions of the ASME: Journal of Tribology, 111, 188-191.
- Christensen, H., & Tonder, K. (1971). The Hydrodynamic Lubrication of Rough Bearing Surfaces of Finite Width. Transactions of the ASME: Journal of Lubrication Technology, 93, 324-330.
- Daly, D. A. (1965). Factors Controlling Traction Between Webs and Their Carrying Rolls. TAPPI Journal, 48, 88A-90A.
- Elrod, H. G. (1973). Thin-Film Lubrication Theory for Newtonian Fluids with Surfaces Possessing Striated Roughness or Grooving. Transactions of the ASME: Journal of Lubrication Technology, 95, 484-489.
- Eshel, A., & Elrod, H. G., Jr. (1965). The Theory of the Infinitely Wide, Perfectly Flexible, Self-Acting Foil Bearing. Transactions of the ASME: Journal of Basic Engineering, 87, 831-836.
- Gross, W. A., editor (1980). Fluid Film Lubrication. New York: John Wiley & Sons, 482-505.

- Jones, D. P. (1992). Air Entrainment as a Mechanism for Low Traction on Rollers and Poor Stacking of Polyester Film Reels, and Its Reduction. Proceedings of the ASME Winter Annual Meeting, Applied Mechanics Division, 149, 123-131.
- Knox, K. L., & Sweeney, T. L. (1971). Fluid Effects Associated with Web Handling. Ind. Eng. Chem. Process. Design. Dev., 10, 201-205.
- Kragelskii, I. V. (1965). Friction and Wear. Washington, D. C.: Butterworths.
- Licht, L. (1968). An Experimental Study of Elastohydrodynamic Lubrication of Foil Bearings. Transactions of the ASME: Journal of Lubrication Technology, 90, 199-220.
- Ma, J. T. S. (1965). An Investigation of Self-Acting Foil Bearings. Transactions of the ASME: Journal of Basic Engineering, 87, 837-846.
- Patir, N., & Cheng, H. S. (1978). An Average Flow Model for Determining Effects of Three-Dimensional Roughness on Partial Hydrodynamic Lubrication. Transactions of the ASME: Journal of Lubrication Technology, 100, 12-17.
- Patir, N., & Cheng, H. S. (1979). Application of Average Flow Model to Lubrication Between Rough Sliding Surfaces. Transactions of the ASME: Journal of Lubrication Technology, 101, 220-230.
- Rabinowicz, E. (1965). Friction and Wear of Materials. New York: John Wiley & Sons
- Sarkar, A. D. (1980). Friction and Wear. New York: Academic Press.
- Tonder, K. (1980). Simulation of the Lubrication of Isotropically Rough Surfaces. ASLE Transactions, 23, 326-333.
- Tonder, K. (1984). A Numerical Assessment of the Effect of Striated Roughness on Gas Lubrication. Transactions of the ASME: Journal of Tribology, 106, 315-319.
- Tonder, K. (1985a). The Construction of Reynolds-Type Equations for Rough Surfaces. Proceedings of the JSLE International Tribology Conference, July 8-10, 1985, Tokyo, Japan, 229-236.
- Tonder, K. (1985b). Theory of Effects of Striated Roughness on Gas Lubrication. Proceedings of the JSLE International Tribology Conference, July 8-10, 1985, Tokyo, Japan, 761-766.
- White, J. W. (1980). Surface Roughness Effects on the Load Carrying Capacity of Very Thin Compressible Lubricating Films. Transactions of the ASME: Journal of Lubrication Technology, 102, 445-451.
- White, J. W. (1983). The Effect of Two-Sided Surface Roughness on Ultra-Thin Gas Films. Transactions of the ASME: Journal of Lubrication Technology, 105, 131-137.
- Ducotey, K. (1993). Traction between Webs and Rollers in Web Handling Applications. Ph.D. Dissertation, Oklahoma State University.



## APPENDIXES

**APPENDIX A**  
**COMPUTER PROGRAMS**

```
100 REM THIS IS A GWBASIC PROGRAM TO DETERMINE THE NECESSARY
110 REM GROOVE FRACTION TO MAINTAIN TRACTION FOR THE HEIGHT
120 REM DEPENDENT MODEL
130 OPEN #1, "0", "HGT.DAT"
140 FOR I = 1 TO 10
150 DGH1 = 10.*I
160 FOR J = 1 TO 41
170 H2H1 = 1. + 0.1*(I - 1)
180 FG = (H2H1 - 1)/DGH1
190 PRINT H2H1,FG,DGH1
200 PRINT #1, H2H1, FG, DGH1
210 NEXT J
215 PRINT
216 PRINT #1
220 NEXT I
230 CLOSE #1
240 END
```

```
100 REM THIS IS A GWBASIC PROGRAM TO DETERMINE THE NECESSARY
110 REM GROOVE FRACTION TO MAINTAIN TRACTION FOR THE LINEAR
120 REM PROBABILITY DISTRIBUTION
130 OPEN #1, "0", "LINFG.DAT"
135 H1S = 0.5
140 FOR I = 1 TO 10
150 DGH1 = 10.*I
155 DGS = DGH1 * H1S
160 FOR J = 1 TO 41
170 H2H1 = 1. + 0.1*(I - 1)
175 H2S = H2H1 * H1S
180 A1 = 1 - DGS - H2S
181 A2 = H2S - H1S
183 A3 = A1^2 - 4 * DGS * A2
184 A4 = A3^0.5
185 FG = 0.5 * (-A1 - A4) / DGS
190 PRINT H2H1,FG,DGH1
200 PRINT #1, H2H1, FG, DGH1
210 NEXT J
215 PRINT
216 PRINT #1
220 NEXT I
230 CLOSE #1
240 END
```

```

' THIS IS A PROGRAM WRITTEN IN QUICKBASIC TO DETERMINE THE
' NECESSARY GROOVE FRACTION TO MAINTAIN TRACTION FOR THE
' LINEAR PROBABILITY DISTRIBUTION
DIM GD(36)
H1R = .0001
OPEN "A:\WEBPROG\GD.DAT" FOR INPUT AS #1
FOR N = 1 TO 36 STEP 1
    INPUT #1, GD(N)
NEXT N
CLOSE #1
OPEN "A:\WEBPROG\GD4.OUT" FOR OUTPUT AS #2
H1N = 3!
FOR I = 1 TO 10
    DGN = 10! * I * H1N
    DGR = 10! * I * H1R
    FOR J = 1 TO 41
        H2R = (1! + .1 * (J - 1)) * H1R
        H2N = (1! + .1 * (J - 1)) * H1N
        X1 = H1N * 10!
        I1 = INT(X1)
        P1A = GD(I1 + 1) + (X1 - I1) * (GD(I1 + 2) - GD(I1 + 1))
        P1 = (1! - P1A)
        FG = 0!
        DELFG = .01
        P2MAX = 0!
        P2 = 0!
        S = .0001
        DO
            H2AN = H2N - FG * DGN
            IF H2AN < 0 THEN
                EXIT DO
            END IF
            X2A = H2AN * 10!
            I2A = INT(X2A)
            IF I2A > 34 THEN
                I2A = 34
            END IF
            P2A = (X2A - I2A) * (GD(I2A + 2) - GD(I2A + 1)) + GD(I2A + 1)
            P2 = (1! - FG) * (1! - P2A)
            R = P2 - P1
            IF P2 > P2MAX THEN
                P2MAX = P2
            END IF
            IF ABS(R) < S THEN
                EXIT DO
            END IF
            IF R < 0 THEN
                IF P2MAX > P2 AND P2 > 0 THEN
                    DELFG = .5 * DELFG
                END IF
                FG = FG + DELFG
            ELSE
                DELFG = .5 * DELFG
                FG = FG - DELFG
            END IF
        LOOP
    NEXT J
NEXT I

```

```
        END IF
    LOOP UNTIL FG > .5
    IF FG > .5 OR H2AN < 0 THEN
        PRINT "There is no possible fg for good traction."
        PRINT #2, "There is no possible fg for good traction."
    ELSE
        RAT = H2R/H1R
        PRINT RAT, FG, DGR
        PRINT #2, RAT, FG, DGR
    END IF
NEXT J
PRINT
PRINT #2, ""
NEXT I
CLOSE #2
END
```

```

C   THIS IS A PROGRAM WRITTEN IN FORTRAN TO DETERMINE THE
C   NECESSARY GROOVE FRACTION TO MAINTAIN TRACTION FOR THE
C   TENSION VARIATION CASE
      DIMENSION GD(36)
      DATA H1R / 0.0001/
      OPEN(5,FILE='GD.DAT')
      DO 50 N=1,36
50  READ(5,*) GD(N)
      CLOSE(5)
      OPEN(4,FILE='GD4.OUT',STATUS='NEW')
      H1N=1.
      T1=1.
      DO 100 I=1,10
      DGN=10.*I*H1N
      DGR=10.*I*H1R
      DO 200 J=1,7
      T2=(11-J)*0.1*T1
      H2R=H1R*(T1/T2)**(2/3)
      H2N=H1N*(T1/T2)**(2/3)
      X1=H1N*10.
      I1=X1/1
      P1A=(GD(I1+1)+(X1-I1)*(GD(I1+2)-GD(I1+1)))
      P1=T1*(1.-P1A)
      FG=0.
      DELFG=0.01
      P2MAX=0.
      P2=0.
      S=0.0001
      DO 210 K=1,1000
      H2AN=H2N-FG*DGN
      IF (H2AN.LT.0.) GO TO 225
      X2A=H2AN*10.
      I2A=X2A/1
      IF (I2A.GT.34) I2A=34
      P2A=(X2A-I2A)*(GD(I2A+2)-GD(I2A+1))+GD(I2A+1)
      P2=T2*(1.-FG)*(1.-P2A)
      R=P2-P1
      IF (P2.GT.P2MAX) P2MAX=P2
      IF (ABS(R).LT.S) GO TO 250
      IF (R.LT.0.) GO TO 225
      DELFG=DELFG*0.5
      FG=FG-DELFG
      GO TO 210
225 IF ((P2MAX.GT.P2).AND.(P2.GT.0.)) DELFG=0.5*DELFG
      FG=FG+DELFG
210 CONTINUE
      WRITE(*,*)'THERE IS NO POSSIBLE FG FOR GOOD TRACTION'
      WRITE(4,*)'THERE IS NO POSSIBLE FG FOR GOOD TRACTION'
      GO TO 200
250 RAT=T1/T2
      WRITE(*,*) RAT,FG,DGR
      WRITE(4,*) RAT,FG,DGR
200 CONTINUE
      WRITE(*,*)

```

```
WRITE(4,*)  
100 CONTINUE  
CLOSE(4)  
STOP  
END
```



**APPENDIX B**

**RAW DATA FOR CALCULATIONS**

## Data from the computer program for the height dependence model

h02/h01	U2/U1	groove fraction, fg			
		dg/h01=10	dg/h01=20	dg/h01=30	dg/h01=40
1.000	1.000	0.00000	0.00000	0.00000	0.00000
1.100	1.154	0.01000	0.00500	0.00333	0.00250
1.200	1.315	0.02000	0.01000	0.00667	0.00500
1.300	1.482	0.03000	0.01500	0.01000	0.00750
1.400	1.657	0.04000	0.02000	0.01333	0.01000
1.500	1.837	0.05000	0.02500	0.01667	0.01250
1.600	2.024	0.06000	0.03000	0.02000	0.01500
1.700	2.217	0.07000	0.03500	0.02333	0.01750
1.800	2.415	0.08000	0.04000	0.02667	0.02000
1.900	2.619	0.09000	0.04500	0.03000	0.02250
2.000	2.828	0.10000	0.05000	0.03333	0.02500
2.100	3.043	0.11000	0.05500	0.03667	0.02750
2.200	3.263	0.12000	0.06000	0.04000	0.03000
2.300	3.488	0.13000	0.06500	0.04333	0.03250
2.400	3.718	0.14000	0.07000	0.04667	0.03500
2.500	3.953	0.15000	0.07500	0.05000	0.03750
2.600	4.192	0.16000	0.08000	0.05333	0.04000
2.700	4.437	0.17000	0.08500	0.05667	0.04250
2.800	4.685	0.18000	0.09000	0.06000	0.04500
2.900	4.939	0.19000	0.09500	0.06333	0.04750
3.000	5.196	0.20000	0.10000	0.06667	0.05000
3.100	5.458	0.21000	0.10500	0.07000	0.05250
3.200	5.724	0.22000	0.11000	0.07333	0.05500
3.300	5.995	0.23000	0.11500	0.07667	0.05750
3.400	6.269	0.24000	0.12000	0.08000	0.06000
3.500	6.548	0.25000	0.12500	0.08333	0.06250
3.600	6.831	0.26000	0.13000	0.08667	0.06500
3.700	7.117	0.27000	0.13500	0.09000	0.06750
3.800	7.408	0.28000	0.14000	0.09333	0.07000
3.900	7.702	0.29000	0.14500	0.09667	0.07250
4.000	8.000	0.30000	0.15000	0.10000	0.07500
4.100	8.302	0.31000	0.15500	0.10333	0.07750
4.200	8.607	0.32000	0.16000	0.10667	0.08000
4.300	8.917	0.33000	0.16500	0.11000	0.08250
4.400	9.230	0.34000	0.17000	0.11333	0.08500
4.500	9.546	0.35000	0.17500	0.11667	0.08750
4.600	9.866	0.36000	0.18000	0.12000	0.09000
4.700	10.189	0.37000	0.18500	0.12333	0.09250
4.800	10.516	0.38000	0.19000	0.12667	0.09500
4.900	10.847	0.39000	0.19500	0.13000	0.09750
5.000	11.180	0.40000	0.20000	0.13333	0.10000

dg/h01=50	dg/h01=60	groove fraction, fg		dg/h01=90	dg/h01=100
		dg/h01=70	dg/h01=80		
0.00000	0.00000	0.00000	0.00000	0.00000	0.00000
0.00200	0.00167	0.00143	0.00125	0.00111	0.00100
0.00400	0.00333	0.00286	0.00250	0.00222	0.00200
0.00600	0.00500	0.00429	0.00375	0.00333	0.00300
0.00800	0.00667	0.00571	0.00500	0.00444	0.00400
0.01000	0.00833	0.00714	0.00625	0.00556	0.00500
0.01200	0.01000	0.00857	0.00750	0.00667	0.00600
0.01400	0.01167	0.01000	0.00875	0.00778	0.00700
0.01600	0.01333	0.01143	0.01000	0.00889	0.00800
0.01800	0.01500	0.01286	0.01125	0.01000	0.00900
0.02000	0.01667	0.01429	0.01250	0.01111	0.01000
0.02200	0.01833	0.01571	0.01375	0.01222	0.01100
0.02400	0.02000	0.01714	0.01500	0.01333	0.01200
0.02600	0.02167	0.01857	0.01625	0.01444	0.01300
0.02800	0.02333	0.02000	0.01750	0.01556	0.01400
0.03000	0.02500	0.02143	0.01875	0.01667	0.01500
0.03200	0.02667	0.02286	0.02000	0.01778	0.01600
0.03400	0.02833	0.02429	0.02125	0.01889	0.01700
0.03600	0.03000	0.02571	0.02250	0.02000	0.01800
0.03800	0.03167	0.02714	0.02375	0.02111	0.01900
0.04000	0.03333	0.02857	0.02500	0.02222	0.02000
0.04200	0.03500	0.03000	0.02625	0.02333	0.02100
0.04400	0.03667	0.03143	0.02750	0.02444	0.02200
0.04600	0.03833	0.03286	0.02875	0.02556	0.02300
0.04800	0.04000	0.03429	0.03000	0.02667	0.02400
0.05000	0.04167	0.03571	0.03125	0.02778	0.02500
0.05200	0.04333	0.03714	0.03250	0.02889	0.02600
0.05400	0.04500	0.03857	0.03375	0.03000	0.02700
0.05600	0.04667	0.04000	0.03500	0.03111	0.02800
0.05800	0.04833	0.04143	0.03625	0.03222	0.02900
0.06000	0.05000	0.04286	0.03750	0.03333	0.03000
0.06200	0.05167	0.04429	0.03875	0.03444	0.03100
0.06400	0.05333	0.04571	0.04000	0.03556	0.03200
0.06600	0.05500	0.04714	0.04125	0.03667	0.03300
0.06800	0.05667	0.04857	0.04250	0.03778	0.03400
0.07000	0.05833	0.05000	0.04375	0.03889	0.03500
0.07200	0.06000	0.05143	0.04500	0.04000	0.03600
0.07400	0.06167	0.05286	0.04625	0.04111	0.03700
0.07600	0.06333	0.05429	0.04750	0.04222	0.03800
0.07800	0.06500	0.05571	0.04875	0.04333	0.03900
0.08000	0.06667	0.05714	0.05000	0.04444	0.04000

## Data from the computer program for the linear probability distribution

h02/h01	U2/U1	groove fraction, fg			
		dg/h01=10	dg/h01=20	dg/h01=30	dg/h01=40
1.000	1.000	0e+0	0e+0	0e+0	0e+0
1.100	1.154	1.112504e-2	5.264664e-3	3.448709e-3	2.564287e-3
1.200	1.315	2.227864e-2	1.053228e-2	6.898245e-3	5.128574e-3
1.300	1.482	3.34621e-2	1.580296e-2	1.034864e-2	7.693815e-3
1.400	1.657	4.467664e-2	2.107663e-2	1.379989e-2	1.025915e-2
1.500	1.837	5.592365e-2	2.635341e-2	1.725184e-2	1.282501e-2
1.600	2.024	6.720462e-2	3.163333e-2	2.070481e-2	1.539078e-2
1.700	2.217	7.852121e-2	3.691659e-2	2.415857e-2	1.795707e-2
1.800	2.415	8.987502e-2	4.220309e-2	2.76132e-2	2.052398e-2
1.900	2.619	1.012679e-1	4.749308e-2	3.10689e-2	2.309094e-2
2.000	2.828	1.127017e-1	5.27864e-2	3.452533e-2	2.565842e-2
2.100	3.043	1.241785e-1	5.808335e-2	3.798294e-2	2.822619e-2
2.200	3.263	1.357007e-1	6.338363e-2	4.144115e-2	3.079453e-2
2.300	3.488	1.472705e-1	6.868782e-2	4.490042e-2	3.336287e-2
2.400	3.718	1.588906e-1	7.399545e-2	4.836064e-2	3.593178e-2
2.500	3.953	1.705639e-1	7.930689e-2	5.182181e-2	3.850112e-2
2.600	4.192	1.822932e-1	8.462229e-2	5.528406e-2	4.107075e-2
2.700	4.437	1.940821e-1	8.994154e-2	5.874717e-2	4.364085e-2
2.800	4.685	2.059342e-1	9.526481e-2	6.221142e-2	4.621129e-2
2.900	4.939	2.158533e-1	1.005922e-1	6.567653e-2	4.878206e-2
3.000	5.196	2.298438e-1	1.059238e-1	6.91427e-2	5.135341e-2
3.100	5.458	2.419106e-1	1.112594e-1	7.26099e-2	5.391494e-2
3.200	5.724	2.540589e-1	1.165594e-1	7.607813e-2	5.649696e-2
3.300	5.995	2.662945e-1	1.219441e-1	7.954744e-2	5.906968e-2
3.400	6.269	2.78624e-1	1.27293e-1	8.30179e-2	6.164236e-2
3.500	6.548	2.910546e-1	1.326467e-1	8.64893e-2	6.421556e-2
3.600	6.831	3.035945e-1	1.380051e-1	8.996188e-2	6.678925e-2
3.700	7.117	3.162529e-1	1.433682e-1	9.343554e-2	6.936336e-2
3.800	7.408	3.290402e-1	1.487362e-1	9.691035e-2	7.19378e-2
3.900	7.702	3.419684e-1	1.541093e-1	1.003863e-1	7.451291e-2
4.000	8.000	3.550511e-1	1.594875e-1	1.038634e-1	7.708821e-2
4.100	8.302	3.68304e-1	1.64871e-1	1.073417e-1	7.966413e-2
4.200	8.607	3.817458e-1	1.702599e-1	1.108211e-1	8.22402e-2
4.300	8.917	3.953981e-1	1.756542e-1	1.143018e-1	8.481698e-2
4.400	9.230	4.09287e-1	1.810541e-1	1.177836e-1	8.739409e-2
4.500	9.546	4.234436e-1	1.864598e-1	1.212668e-1	8.997168e-2
4.600	9.866	4.379064e-1	1.918715e-1	1.247512e-1	9.124971e-2
4.700	10.189	4.527228e-1	1.97289e-1	1.282368e-1	9.51282e-2
4.800	10.516	4.679536e-1	2.027127e-1	1.317235e-1	9.770718e-2
4.900	10.847	4.836774e-1	2.081428e-1	1.352117e-1	1.002866e-1
5.000	11.180	5.00e-1	2.135792e-1	1.387013e-1	1.028667e-1

groove fraction, fg					
dg/h01=50	dg/h01=60	dg/h01=70	dg/h01=80	dh/h01=90	dg/h01=100
Oe+0	Oe+0	Oe+0	Oe+0	Oe+0	Oe+0
2.040901e-3	1.694902e-3	1.449422e-3	1.265812e-3	1.123683e-3	1.010094e-3
4.082031e-3	3.390026e-3	2.898679e-3	2.531719e-3	2.24745e-3	2.020264e-3
6.123162e-3	5.085214e-3	4.348156e-3	3.797674e-3	3.370921e-3	3.030396e-3
8.164826e-3	6.78037e-3	5.797686e-3	5.063677e-3	4.494689e-3	4.040642e-3
1.020615e-2	8.475749e-3	7.297686e-3	6.32968e-3	5.618414e-3	5.050812e-3
1.2248e-2	1.017122e-2	8.696747e-3	7.595825e-3	6.742351e-3	6.061135e-3
1.429001e-2	1.186679e-2	1.014644e-2	8.86178e-3	7.866075e-3	7.071418e-3
1.633213e-2	1.356243e-2	1.159608e-2	1.012807e-2	8.989716e-3	8.081718e-3
1.837441e-2	1.525831e-2	1.304599e-2	1.139412e-2	1.011357e-2	9.091721e-3
2.041695e-2	1.695423e-2	1.44958e-2	1.266027e-2	1.123742e-2	1.010201e-2
2.24596e-2	1.865018e-2	1.594571e-2	1.392655e-2	1.236131e-2	1.111244e-2
2.450237e-2	2.034623e-2	1.739584e-2	1.51928e-2	1.348512e-2	1.212265e-2
2.654553e-2	2.204231e-2	1.884586e-2	1.645923e-2	1.460932e-2	1.313301e-2
2.858864e-2	2.373874e-2	2.029599e-2	1.772552e-2	1.573313e-2	1.414345e-2
3.063194e-2	2.543504e-2	2.174623e-2	1.8992e-2	1.685723e-2	1.515385e-2
3.267559e-2	2.713153e-2	2.31963e-2	2.025867e-2	1.79813e-2	1.616436e-2
3.471935e-2	2.882802e-2	2.464687e-2	2.1525e-2	1.910536e-2	1.71748e-2
3.676357e-2	3.052473e-2	2.609716e-2	2.279148e-2	2.02296e-2	1.818523e-2
3.880753e-2	3.222154e-2	2.754751e-2	2.40582e-2	2.135362e-2	1.919575e-2
4.085194e-2	3.391842e-2	2.899819e-2	2.532501e-2	2.247772e-2	2.020615e-2
4.28965e-2	3.561554e-2	3.044864e-2	2.659145e-2	2.3602e-2	2.12167e-2
4.494122e-2	3.731273e-2	3.189937e-2	2.785826e-2	2.472623e-2	2.222736e-2
4.698605e-2	3.900983e-2	3.334999e-2	2.912507e-2	2.585047e-2	2.323815e-2
4.903122e-2	4.070727e-2	3.480083e-2	3.039179e-2	2.697479e-2	2.424854e-2
5.103122e-2	4.240465e-2	3.625178e-2	3.16587e-2	2.809906e-2	2.525917e-2
5.312206e-2	4.410229e-2	3.770256e-2	3.292561e-2	2.922346e-2	2.626972e-2
5.516781e-2	4.579996e-2	3.915356e-2	3.419256e-2	3.034783e-2	2.728054e-2
5.721375e-2	4.749782e-2	4.060473e-2	3.549256e-2	3.147219e-2	2.829117e-2
5.92601e-2	4.919567e-2	4.205579e-2	3.672657e-2	3.259663e-2	2.930187e-2
6.130627e-2	5.089375e-2	4.350695e-2	3.799362e-2	3.372116e-2	3.031265e-2
6.335282e-2	5.25919e-2	4.495817e-2	3.926087e-2	3.484552e-2	3.132336e-2
6.539959e-2	5.429014e-2	4.640955e-2	4.05282e-2	3.597014e-2	3.233414e-2
6.744648e-2	5.59885e-2	4.786099e-2	4.17953e-2	3.709471e-2	3.334492e-2
6.949371e-2	5.768691e-2	4.931249e-2	4.036245e-2	3.821941e-2	3.435589e-2
7.154103e-2	5.938565e-2	5.076409e-2	4.432984e-2	3.934403e-2	3.536663e-2
7.358864e-2	6.108446e-2	5.221569e-2	4.559722e-2	4.046856e-2	3.637745e-2
7.563656e-2	6.278318e-2	5.36674e-2	4.68647e-2	4.159338e-2	3.738838e-2
7.768467e-2	6.448225e-2	5.511911e-2	4.813214e-2	4.2718e-2	3.839943e-2
7.973278e-2	6.618118e-2	5.657093e-2	4.939957e-2	4.384287e-2	3.941032e-2
8.178139e-2	6.788044e-2	5.80228e-2	5.066719e-2	4.496765e-2	4.042133e-2

## Data from the computer program for the Gaussian roughness distribution

h02/h01	U2/U1	groove fraction, fg			
		dg/h01=10	dg/h01=20	dg/h01=30	dg/h01=40
1e+0	1.000	0e+0	0e+0	0e+0	0e+0
1.1e+0	1.154	1.070312e-2	5.195312e-3	3.417968e-3	2.558594e-3
1.2e+0	1.315	2.140625e-2	1.035156e-2	6.835937e-3	5.097656e-3
1.3e+0	1.482	3.21875e-2	1.554687e-2	1.025391e-2	7.65625e-3
1.4e+0	1.657	4.296875e-2	2.074219e-2	1.367187e-2	1.019531e-2
1.5e+0	1.837	5.374999e-2	2.59375e-2	1.708984e-2	1.27539e-2
1.6e+0	2.024	6.453124e-2	3.109375e-2	2.050781e-2	1.529297e-2
1.7e+0	2.217	7.531249e-2	3.628906e-2	2.394531e-2	1.785156e-2
1.8e+0	2.415	8.617187e-2	4.148437e-2	2.734375e-2	2.041016e-2
1.9e+0	2.619	9.703123e-2	4.667969e-2	3.078125e-2	2.294922e-2
2e+0	2.828	1.078906e-1	5.1875e-2	3.419922e-2	2.550781e-2
2.1e+0	3.043	1.188281e-1	5.710937e-2	3.761719e-2	2.804687e-2
2.2e+0	3.263	1.296875e-1	6.230468e-2	4.105468e-2	3.060547e-2
2.3e+0	3.488	1.40625e-1	6.749999e-2	4.447265e-2	3.316406e-2
2.4e+0	3.718	1.515625e-1	7.273436e-2	4.789062e-2	3.572266e-2
2.5e+0	3.953	1.624219e-1	7.792968e-2	5.132812e-2	3.826172e-2
2.6e+0	4.192	1.733594e-1	8.312499e-2	5.474608e-2	4.082031e-2
2.7e+0	4.437	1.84375e-1	8.835936e-2	5.816406e-2	4.33789e-2
2.8e+0	4.685	1.953125e-1	9.359374e-2	6.160155e-2	4.59375e-2
2.9e+0	4.939	2.064063e-1	9.878904e-2	6.503905e-2	4.847656e-2
3e+0	5.196	2.174219e-1	1.040234e-1	6.845702e-2	5.103515e-2
3.1e+0	5.458	2.285157e-1	1.092578e-1	7.189452e-2	5.359374e-2
3.2e+0	5.724	2.396875e-1	1.144531e-1	7.531249e-2	5.615234e-2
3.3e+0	5.995	2.507813e-1	1.196875e-1	7.874998e-2	5.871094e-2
3.4e+0	6.269	2.61875e-1	1.249219e-1	8.218749e-2	6.124999e-2
3.5e+0	6.548	2.729686e-1	1.301562e-1	8.562499e-2	6.380858e-2
3.6e+0	6.831	2.842186e-1	1.353906e-1	8.906248e-2	6.636717e-2
3.7e+0	7.117	2.953906e-1	1.40625e-1	9.249999e-2	6.892577e-2
3.8e+0	7.408	3.067187e-1	1.458203e-1	9.591795e-2	7.148436e-2
3.9e+0	7.702	3.179687e-1	1.510547e-1	9.935545e-2	7.404295e-2
4e+0	8.000	3.29375e-1	1.562891e-1	1.027929e-1	7.660155e-2
4.1e+0	8.302	3.407031e-1	1.615234e-1	1.062305e-1	7.916015e-2
4.2e+0	8.607	3.520312e-1	1.667578e-1	1.096679e-1	8.171874e-2
4.3e+0	8.917	3.635156e-1	1.719922e-1	1.13125e-1	8.427733e-2
4.4e+0	9.230	3.749999e-1	1.772656e-1	1.165625e-1	8.683593e-2
4.5e+0	9.546	3.865624e-1	1.825e-1	1.2e-1	8.939451e-2
4.6e+0	9.866	3.981249e-1	1.877344e-1	1.234375e-1	9.195311e-2
4.7e+0	10.189	4.098437e-1	1.930078e-1	1.268554e-1	9.45117e-2
4.8e+0	10.516	4.214842e-1	1.982422e-1	1.30293e-1	9.707029e-2
4.9e+0	10.847	4.33203e-1	2.035157e-1	1.337305e-1	9.962889e-2
5e+0	11.180	4.449998e-1	2.087891e-1	1.37168e-1	1.021875e-1

dg/h01=50	dg/h01=60	groove fraction, fg		dg/h01=90	dg/h01=100
		dg/h01=70	dg/h01=80		
0e+0	0e+0	0e+0	0e+0	0e+0	0e+0
2.03125e-3	1.689453e-3	1.445313e-3	1.269531e-3	1.123047e-3	1.010742e-3
4.0625e-3	3.378906e-3	2.890625e-3	2.529297e-3	2.246094e-3	2.021484e-3
6.09375e-3	5.078125e-3	4.335937e-3	3.798828e-3	3.36914e-3	3.027344e-3
8.125e-3	6.757812e-3	5.791015e-3	5.058594e-3	4.492188e-3	4.042969e-3
1.016601e-2	8.45703e-3	7.236328e-3	6.328125e-3	5.615234e-3	5.048828e-3
1.220703e-2	1.014648e-2	8.681639e-3	7.58789e-3	6.73828e-3	6.064453e-3
1.423828e-2	1.183594e-2	1.012695e-2	8.857423e-3	7.861328e-3	7.070312e-3
1.626953e-2	1.352539e-2	1.158203e-2	1.011719e-2	8.984376e-3	8.085937e-3
1.830078e-2	1.521484e-2	1.302734e-2	1.138672e-2	1.010742e-2	9.091797e-3
2.033203e-2	1.691406e-2	1.447266e-2	1.264648e-2	1.123047e-2	1.010254e-2
2.236328e-2	1.860351e-2	1.591797e-2	1.391601e-2	1.235351e-2	1.111328e-2
2.440429e-2	2.029297e-2	1.736328e-2	1.517578e-2	1.347656e-2	1.212402e-2
2.644531e-2	2.198242e-2	1.881836e-2	1.644531e-2	1.459961e-2	1.313476e-2
2.847656e-2	2.367187e-2	2.026367e-2	1.770508e-2	1.572754e-2	1.414062e-2
3.050781e-2	2.537109e-2	2.170898e-2	1.897461e-2	1.685547e-2	1.515625e-2
3.253906e-2	2.706054e-2	2.316406e-2	2.024414e-2	1.797852e-2	1.616211e-2
3.458008e-2	2.875e-2	2.460937e-2	2.15039e-2	1.910156e-2	1.717773e-2
3.662109e-2	3.044922e-2	2.605469e-2	2.277344e-2	2.022461e-2	1.818359e-2
3.865235e-2	3.213867e-2	2.75e-2	2.40332e-2	2.134765e-2	1.919922e-2
4.068359e-2	3.382812e-2	2.894531e-2	2.530273e-2	2.24707e-2	2.020508e-2
4.272461e-2	3.552735e-2	3.040039e-2	2.65625e-2	2.359375e-2	2.12207e-2
4.476562e-2	3.721679e-2	3.184571e-2	2.783203e-2	2.471679e-2	2.222656e-2
4.679688e-2	3.890625e-2	3.329102e-2	2.910156e-2	2.583984e-2	2.324219e-2
4.882812e-2	4.060547e-2	3.474609e-2	3.036133e-2	2.696289e-2	2.424804e-2
5.086914e-2	4.229492e-2	3.619141e-2	3.163086e-2	2.808594e-2	2.526367e-2
5.291015e-2	4.398437e-2	3.763672e-2	3.289062e-2	2.920898e-2	2.626953e-2
5.49414e-2	4.568359e-2	3.909179e-2	3.416015e-2	3.033691e-2	2.728515e-2
5.697265e-2	4.737305e-2	4.053711e-2	3.542969e-2	3.146484e-2	2.829101e-2
5.902344e-2	4.90625e-2	4.198242e-2	3.668946e-2	3.258789e-2	2.930664e-2
6.105468e-2	5.076171e-2	4.34375e-2	3.795898e-2	3.371094e-2	3.03125e-2
6.308594e-2	5.245117e-2	4.488281e-2	3.922852e-2	3.483398e-2	3.132812e-2
6.51367e-2	5.414062e-2	4.632812e-2	4.048828e-2	3.595703e-2	3.233398e-2
6.716795e-2	5.583984e-2	4.778321e-2	4.175781e-2	3.708008e-2	3.334961e-2
6.91992e-2	5.752929e-2	4.922852e-2	4.301758e-2	3.820312e-2	3.435547e-2
7.124999e-2	5.921875e-2	5.068359e-2	4.42871e-2	3.932617e-2	3.537109e-2
7.328124e-2	6.091796e-2	5.21289e-2	4.555665e-2	4.044922e-2	3.637696e-2
7.531249e-2	6.261718e-2	5.357421e-2	4.681641e-2	4.158203e-2	3.739258e-2
7.736327e-2	6.430664e-2	5.502929e-2	4.808594e-2	4.270508e-2	3.839844e-2
7.939451e-2	6.599608e-2	5.647461e-2	4.935547e-2	4.382812e-2	3.941406e-2
8.14453e-2	6.76953e-2	5.792968e-2	5.061523e-2	4.495117e-2	4.04248e-2

## Data from the computer program for the tension variation condition

T2/T1	groove fraction, fg				
	dg/h01=10	dg/h01=20	dg/h01=30	dg/h01=40	dg/h01=50
1e+0	0e+0	0e+0	0e+0	0e+0	0e+0
1.111111e+0	1.5375e-2	7.375e-3	4.875e-3	3.625e-3	2.890625e-3
1.25e+0	3.375e-2	1.625e-2	1.06875e-2	7.96875e-3	6.359375e-3
1.428571e+0	5.649996e-2	2.70625e-2	1.778125e-2	1.325e-2	1.05625e-2
1.666667e+0	8.525e-2	4.068749e-2	2.671875e-2	1.990625e-2	1.584375e-2
2e+0	1.240001e-1	5.862496e-2	3.843749e-2	2.859375e-2	2.278125e-2
2.5e+0	1.812502e-1	8.4125e-2	5.499996e-2	4.084374e-2	3.25e-2
	groove fraction, fg				
dg/h01=60	dg/h01=70	dg/h01=80	dg/h01=90	dg/h01=100	
0e+0	0e+0	0e+0	0e+0	0e+0	
2.40625e-3	2.0625e-3	1.796875e-3	1.601562e-3	1.4375e-3	
5.28125e-3	4.515626e-3	3.953125e-3	3.507813e-3	3.15625e-3	
8.781251e-3	7.515626e-3	6.562501e-3	5.828125e-3	5.242188e-3	
1.317188e-2	1.126563e-2	9.84375e-3	8.734374e-3	7.859374e-3	
1.892188e-2	1.617188e-2	1.414063e-2	1.254688e-2	1.128125e-2	
2.696875e-2	2.30625e-2	2.014063e-2	1.7875e-2	1.60625e-2	



**VITA**

**Benjamin Alan Funk**

**Candidate for the Degree of**

**Master of Science**

**Thesis: THEORETICAL MODELING OF THE EFFECTS OF ROUGHNESS AND GROOVING ON THE TRACTION AND FILM HEIGHT IN WEB HANDLING SYSTEMS**

**Major Field: Mechanical Engineering**

**Biographical:**

**Personal Data: Born in Monterrey, California, October 9, 1968, the son of Ronald C. and Marilyn J. Funk.**

**Education: Graduated from Norman High School, Norman, Oklahoma, in May, 1986; received Bachelor of Science Degree in Engineering and Applied Science from California Institute of Technology in June, 1990; completed requirements for the Master of Science Degree at Oklahoma State University in December, 1993.**

**Professional Experience: Teaching Assistant, Department of Mechanical and Aerospace Engineering, Oklahoma State University, August, 1990, to May, 1991; Research Assistant, Department of Mechanical and Aerospace Engineering, Oklahoma State University, May, 1991, to July, 1993.**